AN EVALUATION OF THE FIRE RESISTIVE QUALITIES OF WALL ASSEMBLIES WITH GYPSUM WALLBOARD MEMBRANES

A Thesis

Presented in Partial Fulfillment of the Requirements for the Degree Master of Science

by

Danny Dale Farmer, B.S.

The Ohio State University
1973

Approved by

Advisor
Department of Civil Engineering

ACKNOWLEDGEMENT

I wish to express my sincere appreciation to my advisor, Professor Richard W. Bletzacker, for suggesting the topic of this study and for his advice throughout the development of this thesis. Gratitude is expressed to Professor Lester F. Smith for his interest and suggestions during this project.

I would like to thank the Building Research Laboratory of The Ohio State University for making their fire test files available for my use. I wish to acknowledge The Ohio State Computer Center for providing the computer time required for the theoretical computations.

Special thanks are extended to Mrs. Shelley Beall and Miss Candace Hauser for typing this thesis.

Finally, I wish to thank my parents and friends for their patience and encouragement throughout this program of graduate study.

TABLE OF CONTENTS

LIST OF TABLES

LIST OF FIGURES

NOMENCLATURE

A, (A_2, A_1, A_2, A_3, A_4)	Area normal to the heat flow path (of components i, 1, 2, 3, and 4, respectively).
AVG	Allowable average unexposed surface temperature exceeded.
b_f, (b_1, b_2, b_3,)	Width of spline flange (of spline component widths 1, 2, and 3, respectively).
C_1, C_2, C_3, C_4	Coefficients of assumed cubic equation.
c_p	Specific heat.
CW	Cotton waste ignition.
E	Simplifying variable.
erf (X)	Error function; probability integral.
erfc (X)	1 - erf (X).
f	Function.
h	Surface heat transfer coefficient.
k	Thermal conductivity.
L, (L_i, L_1, L_2, L_3)	Thickness of solid medium (of components i, 1, 2, and 3, respectively).
L_c	Thickness of stud cavity.

L_g	Thickness of gypsum wallboard layer(s).
L_R	Thickness of room side core.
L_S	Thickness of shaft side core.
L_{std}	Depth of stud.
L_T	Total thickness of transformed homogeneous medium.
LD	Load failure of load bearing assembly.
n	Positive integer.
p	Simplifying variable.
P	Steel stud partition assembly.
q	Energy flux.
r	Simplifying variable for integration by parts.
R, (R_i, R_1, R_2 R_3, R_4)	Resistance to conductive heat transfer; thermal resistance (of components i, 1, 2, 3, and 4, respectively).
R_T	Thermal resistance of transformed homogeneous medium.
s	Simplifying variable for integration by parts.
S	Steel spline shaft wall assembly.
SHT	Allowable single high unexposed surface temperature exceeded.
t	Elapsed time of heat exposure.
T, T_i	Temperature, degrees Fahrenheit (initial temperature).

T_1	Transient temperature.
T_A	Ambient temperature.
T_E	Exposed surface temperature.
T_F	Furnace temperature.
T_H	Relatively high temperature region.
T_L	Relatively low temperature region.
T_U	Unexposed surface temperature.
u	Portion of solution for steady state conditions.
v	Portion of solution by Duhamel's theorem for transient conditions.
w	Eigenvalue.
W	Wood stud wall assembly.
x, y, z	Orthogonal reference axes, associated with the energy flow path.
X	Simplifying variable.
α	Thermal diffusivity.
α_i, α_1, α_2, α_3	Mean thermal diffusivity (of components i, 1, 2, and 3, respectively).
α_g	Mean thermal diffusivity of gypsum wall-board.

α_r	Reduced thermal diffusivity.
α_R	Mean thermal diffusivity of room side core.
α_S	Mean thermal diffusivity of shaft side core.
α_{std}	Mean thermal diffusivity of stud.
α_T	Transformed mean thermal diffusivity.
ρ	Density of medium.

CHAPTER I
INTRODUCTION

Wall assemblies consisting of gypsum wallboard membranes have long been basic systems in building construction. In order that these assemblies be used in construction, however, they must meet performance requirements in accordance with the building code authority having jurisdiction at the proposed building site. The codes recognize that fire safety is an essential structural feature. To insure that a building is designed with a balanced network of fire resistive components and to insure that neighboring buildings are not endangered, a nationally recognized standard test method was established to prescribe the fire endurance classification of building systems. The American Society for Testing and Materials issued the Standard Methods of Fire Tests of Building Construction and Materials, ASTM Designation E 119, in an attempt to promote uniformity of requirements of the building code authorities in the United States. The methods require that an assembly, representative of field construction, be exposed to a fire of prescribed severity, following as closely as possible the Standard ASTM Time-Temperature Curve. [1*] Performance is defined as the period of resistance to the standard fire exposure elapsing before the first critical end point criterion is reached.

This investigation is restricted to wall and partition assemblies utilizing gypsum wallboard membranes. The research data is compiled from ASTM E 119 fire tests performed and reported by the Building ResearchLaboratory of The Ohio State University on specimens constructed by and under the supervision of the fire test clients.

The sponsoring companies are concerned in marketing construction materials which they may manufacture or distribute. Therefore, one of the clients' goals is to design an assembly which will demonstrate an ASTM Fire Endurance Classification consistent with their marketing needs. This investigation will examine the thermal properties of the materials of construction of the sponsored fire tests, with particular emphasis on the gypsum wallboard membranes. An electrical resistance analogue is implemented to determine the relevant thermal properties of composite walls.

A theoretical equation applying Duhamel's theorem for transient boundary conditions was derived to compare the unexposed surface temperatures from the fire test results with theoretical values. The theoretical

---

*Superscripted numbers indicate corresponding references in bibliography.

equation produces an unexposed surface temperature history of the fire test specimen as a function of the thermal properties, elapsed time and the assumed exposed temperature history. Graphs are prepared which may assist in the design of a wall assembly with gypsum wallboard membranes in anticipation of a fire test.

CHAPTER 2
DESCRIPTION OF THE TEST SPECIMENS, TEST PROCEDURE, AND FIRE TEST RESULTS

The building materials which comprised the test specimens treated in this investigation were varied. The materials of construction are described in generic terms and tradenames are excluded. The list of materials used in the specimen construction in addition to gypsum wallboard included studs with accompanying perimeter framing, membrane fasteners, mineral fiber insulation, and joint treatment.

Gypsum wallboard consists primarily of a gypsum core, with or without fibers, and porous paper bonded to the core. Gypsum wallboard is used essentially as an interior surfacing for building structures. The gypsum wallboard used in the building industry is termed "regular", Type "X", Type "XX", or Type "XXX". The "regular" wallboard and Type "X" are the only types defined in ASTM Specifications (ASTM Designation C-36).

Type "XX" and Type "XXX" are terms produced by manufacturers to represent products whose properties differ from ASTM designations. The Type "X" gypsum wallboard is manufactured to provide specific fire-resistive characteristics; the structural integrity of the wallboard is also improved because the fibrous materials reinforce the wallboard and counter the tendency to shrink. The nominal thickness of the wallboard ranges from 1/4 in. to 5/8 in. in 1/8 in. increments. Gypsum coreboard, however, is supplied in a nominal 1 in. thickness. The wallboard panel width ranges from 16 in. to 48 in. and the length from 4 ft to 16 ft. The longitudinal edges of the wallboard are either plain, recessed, or tapered to receive a joint reinforcing strip and compound. The average weight of the wallboard per 1, 000 sq ft was measured and recorded during construction of the test specimens.

The studs used were either steel or wood studs. The steel studs were cold formed from light gage steel with a carbon content of less than 0.5 percent with an approximate thickness ranging from 0. 021 in. to 0. 036 in. including a galvanized coating. In all test specimens considered, the steel studs were used in non-load bearing partitions or shaft wall assemblies. The nominal length of the steel studs was 10 ft in general.

The wood studs were used in both non-load bearing partitions and load bearing wall assemblies. The wood was of a coniferous variety such as Douglas Fir or Southern Pine. The moisture content of the wood studs was determined by an electrical resistance moisture meter to assure that the moisture content was below the limit prescribed by ASTM Specifications.

The fasteners used were screws, nails, or wallboard clips. For recording purposes, the type of fastener with pertinent dimensions and the fastener spacing in the test assembly were listed during construction.

The joint treatment, consisting of joint compound and joint reinforcing tape, was used to conceal the wallboard joints and to prepare the wall for what would be wall decoration in field construction. Battens had limited use on the test specimens where joint compound and joint tape were not implemented.

Low temperature insulation (exclusive of asbestos and similar high temperature insulations) was utilized for sound isolation and vapor control. The insulation was usually supplied in fibrous mineral blankets suitable for friction fit installation into the stud cavities. The density and nominal dimensions of the insulation were determined and recorded.

Construction of the test specimens was performed by skilled workmen employed by and under the direct supervision of the fire test client. The specimens considered were steel stud partitions, steel spline unsymmetrical shaft walls, and wood stud partitions and load bearing wall assemblies. The number and thickness of the wallboard layers were dependent upon the purpose of the assembly or the ASTM Fire Endurance Classification required of the assembly. Following is a description of the construction of a non-load bearing partition assembly faced with one layer of gypsum wallboard on each surface; the remaining types of assemblies considered would be constructed in much the same manner.

Figure 1 shows the concrete frame in which the test assembly is constructed. The bolster is aligned in the concrete yoke to form the proper height for the assembly. The perimeter framing with wallboard protection for the concrete frame is securely anchored at the vertical and top edges. The base stud track is anchored by drive pins.

The studs are positioned across the test frame opening at a predetermined spacing. The wallboard is cut to size and erected with the edges located over the studs. The wallboard for one face is attached to the studs and perimeter tracks with screws driven flush with the surface. Insulation is friction fitted into the stud cavities.

The wallboard for the other face is erected and fastened to the studs and framing in much the same manner. The joints are offset one stud spacing from the opposite surface wallboard joints. Figure 2 shows this assembly during construction.

Variables of construction may include (a) test specimen dimensions, although ASTM E 119 specifies an exposed surface area of 100 sq ft except where field construction would warrent a shorter wall height; (b) gypsum wallboard core formulation and dimensions; (c) stud composition, shape and dimensions; (d) type of membrane fasteners and spacing; (e) density and type of insulation, if used; (f) type of joint treatment; (g) workmanship of construction.

The test furnace consists of masonry walls lined with fire brick. One wall of the furnace is a hinged steel restraining frame in which the

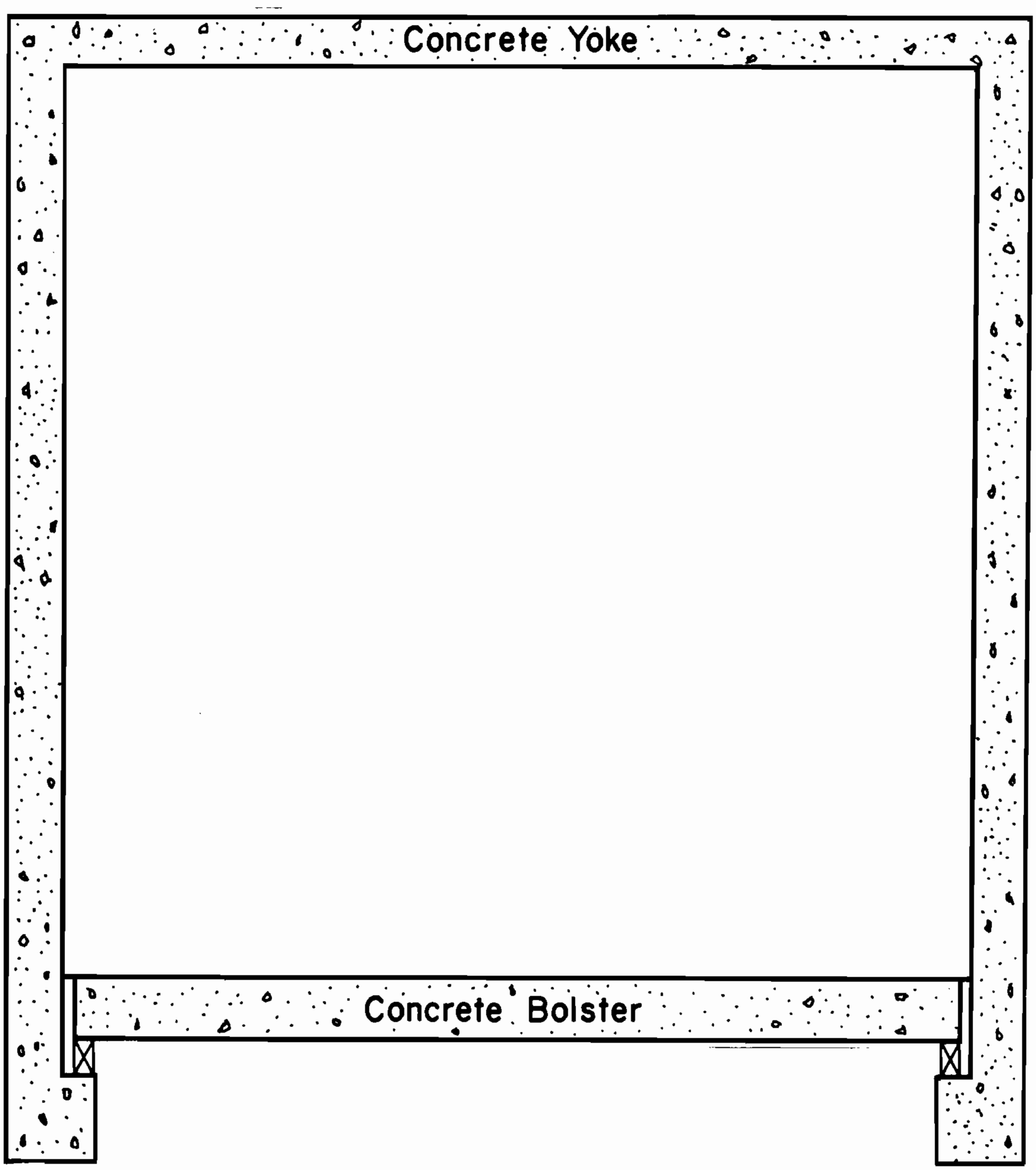

Figure 1. Concrete test frame

Figure 2. Assembly during construction

concrete frame containing the test specimen is placed as shown in Figure 3.

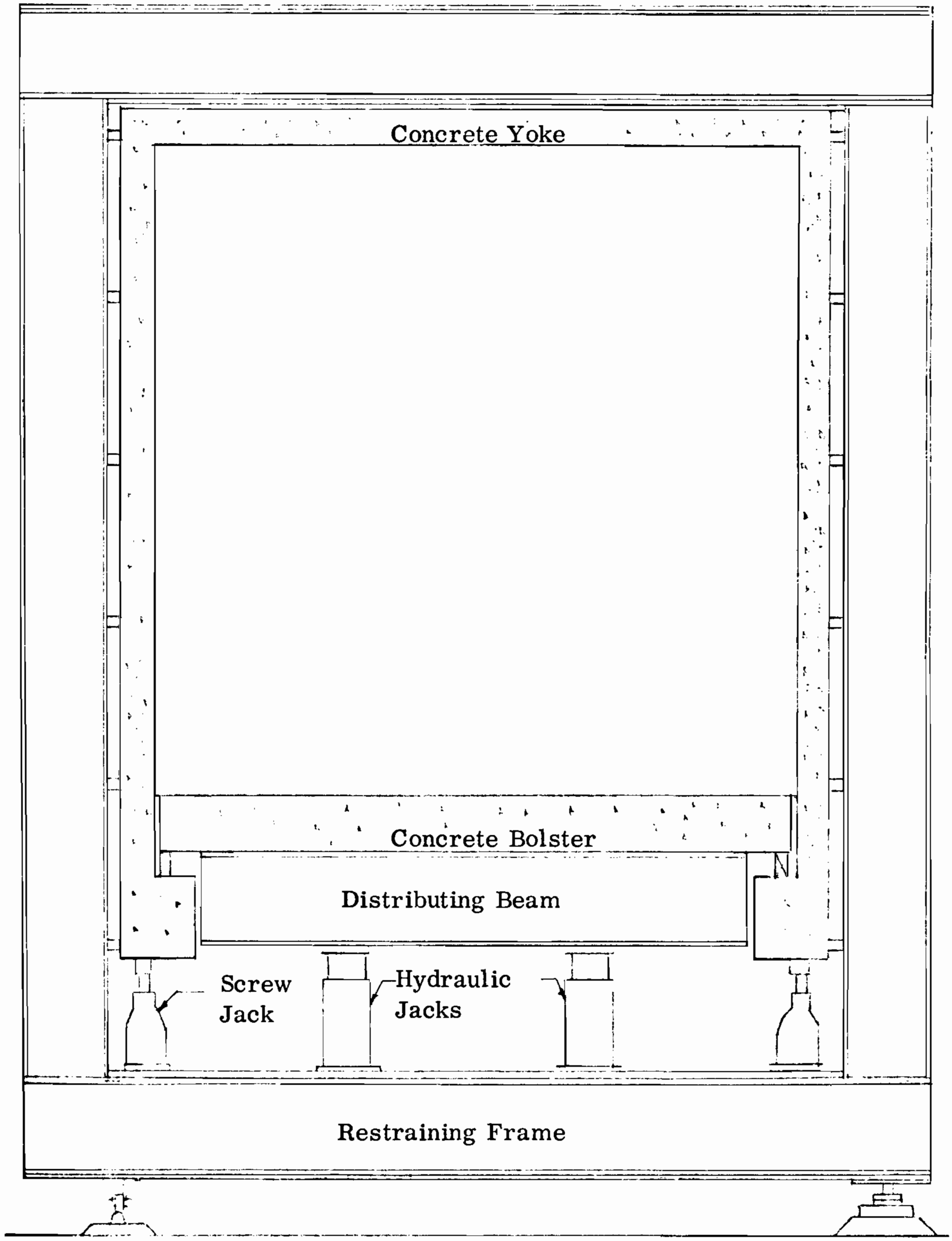

Figure 3. Concrete bolster and test frame arrangement

Ports are located in the two walls adjoining the restraining frame to permit visual observations of the exposed surface of the test specimen. The furnace is fired with ten luminous flame natural gas burners.

The furnace temperature was controlled from the average of ten individual Chromel-Alumel thermocouples enclosed in stainless steel protection tubes within the furnace chamber. The furnace temperature history seldom exceeded 1 percent area variation from the Standard ASTM Time-Temperature Curve, which is shown in Figure 4.

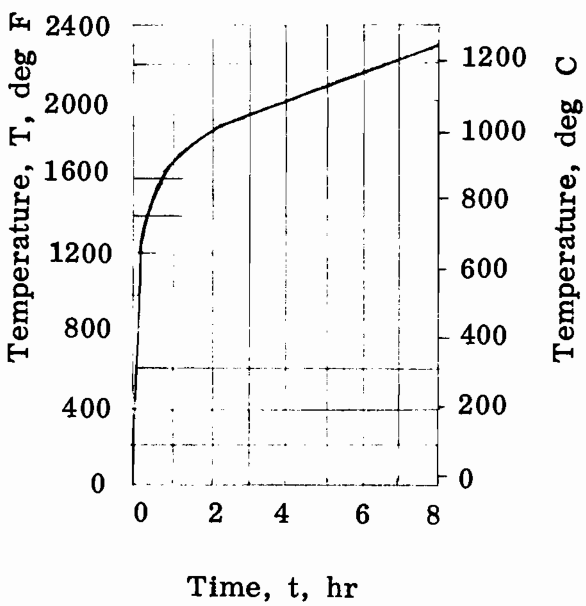

Figure 4. ASTM Time-Temperature Curve

The unexposed surface temperatures were measured with ten thermocouples of Chromel-Alumel wire. Each thermocouple was tightly covered with an oven dried, felted asbestos pad 6 in. square by approximately 0.4 in. thick. The thermocouples were arranged to provide representative readings with respect to the specimen construction.

The furnace and unexposed surface thermocouples were connected to a direct reading temperature indicating instrument and were read at the start of the test and at intervals of not more than 5 minutes thereafter.

The fire endurance test was terminated when any one of the following criteria were met: (a) flame or gases hot enough to ignite cotton waste were passed through the wall or partition; (b) the average unexposed thermocouple temperature raised more than 250°F above its initial temperature, or (c) any one unexposed thermocouple temperature raised more than 325°F above its initial temperature; and (d) a load bearing wall failed to sustain the applied load.

The following procedure was employed for the testing of load bearing wall assemblies. The test frame containing the test wall is placed in the test restraining frame. The loading beam is positioned against the concrete bolster. Unlike a non-load bearing assembly, the wall is not restrained at the vertical edges. The load is applied by two 100 ton hydraulic rams. The load was read by means of an electronic load cell placed between the piston head of a 10 ton master ram and a restraining frame. The master ram was energized by the same hydraulic energy source utilized for the 100 ton loading rams. The system was monitored during the test to insure a constant superimposed load.

Each test specimen described was tested in accordance with ASTM E 119. The failure modes are abbreviated as follows:

(a) CW - Cotton waste ignition

(b) AVG - Allowable average unexposed surface temperature exceeded

(c) SHT - Allowable single high unexposed surface temperature exceeded

(d) LD - Load failure of load bearing assembly

Tables 1, 2, and 3 describe the construction and test results of specimens considered in this study. Table 1 is a listing of non-load bearing partition assemblies with steel studs faced with gypsum wallboard. Table 2 lists shaft wall assemblies with steel splines lined with gypsum wallboard. Table 3 is a listing of wall assemblies with wood studs faced with gypsum wallboard.

TABLE 1

PARTITION ASSEMBLIES WITH STEEL STUDS
FACED WITH GYPSUM WALLBOARD

Specimen No.	Exposed Surface Wallboard Type and Thickness (in.)	Stud Shape	Stud Depth, Thickness (in.)	Cavity Material and Thickness (in.)	Unexposed Surface Wallboard Type and Thickness (in.)	Total Thickness of Partition (in.)	Endurance Time (minutes)	Failure Mode, Location.	Time of First Wallboard Fall off (minutes)
P1	1/2 X	Channel	2-1/2, .021	2-1/2 Glass fiber insulation	1/2 X	3-1/2	60	SHT, Stud	None
P2	1/2 X	Channel	2-1/2, .021	2-1/2 Glass fiber insulation	1/2 X	3-1/2	60	SHT, Stud	None
P3	1/2 XXX	Channel	1-1/2	1-1/2 Rock wool	1/2 XXX	2-1/2	61	SHT, Cavity	None
P4	1/2 XXX, 1/2 XXX	I	2, .024	2 Air space	1/2 XXX, 1/2 XXX	4	132	SHT, Stud	None
P5	1/2 XXX	Channel	3-5/8 .021	3-5/8 Air space	1/2 Reg., 1/2 Reg.	5-1/8	120	SHT, Stud	None
P6	5/8 XXX	Channel	2-1/2, .020	2 Mineral wool insulation	5/8 XXX	3-3/4	66	SHT, Stud	None

TABLE 1

(Continued)

Specimen No.	Exposed Surface Wallboard Type and Thickness (in.)	Stud Shape	Stud Depth, Thickness (in.)	Cavity Material and Thickness (in.)	Unexposed Surface Wallboard Type and Thickness (in.)	Total Thickness of Partition (in.)	Endurance Time (minutes)	Failure Mode, Location	Time of First Wallboard Fall off (minutes)
P7	5/8 XXX	Channel	2-1/2, .021	2-1/2 Air space	5/8 XXX	3-3/4	62	SHT, Stud	None
P8	5/8 XXX	Channel	1-3/4	1-3/4 Air space	5/8 XXX	3	60	SHT, Stud	None
P9	5/8 X	Channel	3-5/8	3-5/8 Air space	5/8 X	4-7/8	61	SHT, Stud	None
P10	5/8 X	I	2-3/4	2-3/4 Air space	5/8 X	3-1/2	60	SHT, Cavity	None
P11	1/2 X	Channel	2-1/2	2 Mineral insulation, 7/16 Rigid board	1/2 X	4	63	SHT, Stud	63
P12	1/2 X, 1/2 X	Channel	2-1/2	2-1/2 Air space	1/2 X, 1/2 X	4-1/2	123	SHT, Stud	99

TABLE 1

(Continued)

Specimen No.	Exposed Surface Wallboard Type and Thickness (in.)	Stud Shape	Stud Depth, Thickness (in.)	Cavity Material and Thickness (in.)	Unexposed Surface Wallboard Type and Thickness (in.)	Total Thickness of Partition (in.)	Endurance Time (minutes)	Failure Mode, Location	Time of First Wallboard Fall off (minutes)
P13	5/8 X	Channel	1-5/8	1-5/8 Air space	5/8 X	2-7/8	67	SHT, AVG, Cavity	None
P14	5/8 X	Channel	3-5/8, .022	3-5/8 Air space	5/8 X	4-7/8	70	SHT, AVG, Stud	None
P15	5/8 X, 5/8 X	Channel	3-5/8, .021	3-5/8 Air space	5/8 X	5-3/4	112	SHT, Stud	97
P16	5/8 X	Channel	3-5/8, .021	3-5/8 Air space	5/8 X, 5/8 X	5-3/4	104	SHT, Stud	None
P17	1/2 X 1/2 X	Channel	2-1/2, .021	2-1/2 Air space	1/2 X, 1/2 X	4-1/2	120	SHT, Stud	93
P18	5/8 X	Channel	3-5/8, .021	3-5/8 Glass fiber insulation	5/8 X, 5/8 X	5-1/2	108	SHT, Stud	None

TABLE 1

(Continued)

Specimen No.	Exposed Surface Wallboard Type and Thickness (in.)	Stud Shape	Stud Depth, Thickness (in.)	Cavity Material and Thickness (in.)	Unexposed Surface Wallboard Type and Thickness (in.)	Total Thickness of Partition (in.)	Endurance Time (minutes)	Failure Mode Location	Time of First Wallboard Fall off (minutes)
P19	1/2 X	2 Channels separated by cavity material	2-1/2, .015	1/2 X, 1/2 X, 1/2 X	1/2 X	8-1/2	144	SHT, Cavity	56
P20	5/8 X	Channel	2-1/2 .021	2-1/2 Air space	5/8 X	3-3/4	73	SHT, Stud	None
P21	5/8 X 5/8 X	Channel	2-1/2 .021	2-1/2 Air space	5/8 X, 5/8 X	5	137	SHT, Stud	61
P22	5/8 X 5/8 X	Channel	3-5/8, .021	3-5/8 Air space	5/8 X, 5/8 X	6-1/8	154	SHT, Stud	91
P23	5/8 X	Channel	3-5/8, .021	3-5/8 Air space	5/8 X,	4-7/8	61	SHT, Stud	None
P24	5/8 X	Channel	3-5/8, .021	3-5/8 Air space	5/8 X	4-7/8	61	SHT, Stud	None

TABLE 1

(Continued)

Specimen No.	Exposed Surface Wallboard Type and Thickness (in.)	Stud Shape	Stud Depth Thickness (in.)	Cavity Material and Thickness (in.)	Unexposed Surface Wallboard Type and Thickness (in.)	Total Thickness of Partition (in.)	Endurance Time (minutes)	Failure Mode Location	Time of First Wallboard Fall off (minutes)
P25	5/8 X, 5/8 X	Zee	3-5/8, .036	3-5/8 Air Space	5/8 X, 5/8 X	6-1/8	144	SHT, Stud	75
P26	5/8 X	Channel	1-5/8, .021	1-5/8 Air Space	5/8 X	2-7/8	65	SHT, Cavity	None
P27	5/8 X	Channel	3-5/8, .022	3-5/8 Air Space	5/8 X	4-7/8	68	SHT, Stud	None
P28	5/8 X	Channel	2-1/2, .022	2-1/2 Air Space	5/8 X	3-3/4	67	SHT, Stud	None

TABLE 2
SHAFT WALL ASSEMBLIES WITH STEEL SPLINES
LINED WITH GYPSUM WALLBOARD

			Shaft Side Core	Room Side Core				
Specimen No.	Exposed Surface	Spline Type (See Details, Figure 5)	Wallboard Type and Thickness (in.), Beginning at Surface Membrane	Wallboard Type and Thickness or Spacer and Thickness (in.) Listed in Order of Erection	Total Thickness (in.)	Endurance Time (minutes)	Failure Mode, Location	Time of First Wallboard Fall off (minutes)
S1	Shaft	S-1	1 Reg. coreboard, 1 x 6 Reg. coreboard	1/2 X, 1/2 X	3	120	SHT, Spline	None
S2	Room	S-1	1 Reg. coreboard, 1 x 6 Reg. coreboard	1/2 X, 1/2 X	3	120	SHT, Spline	99
S3	Shaft	S-2	1 Reg. coreboard, 1x6 Reg. coreboard	5/8 X, 5/8 X	3-1/4	136	SHT, Cavity	117
S4	Shaft	S-2	1 Reg. coreboard	5/8 X, 5/8 X, 5/8 X	3-7/8	185	SHT, Spline	137
S5	Shaft	S-1	1 Reg. coreboard, 1x6 Reg. coreboard	1/2 Reg., 1/2 Reg.	3	113	SHT Spline	None

TABLE 2 (Continued)

Specimen No.	Exposed Surface	Spline Type (See Details, Figure 5)	Shaft Side Core: Wallboard Type and Thickness (in.) Beginning at Surface Membrane	Room Side Core: Wallboard Type and Thickness or Spacer and Thickness (in.) Listed in Order of Erection	Total Thickness (in.)	Endurance Time (minutes)	Failure Mode, Location	Time off Wall-board Fall off (minutes)
S6	Shaft	S-1	1 Reg. coreboard, 1 x 6 Reg. coreboard	5/8 X, 5/8 X	3-1/4	122	SHT, Spline	107
S7	Shaft	S-3	1 Reg. coreboard, 5/8 Reg.	5/8 XXX	2-1/4	103	SHT, Spline	None
S8	Shaft	S-3	1 Reg. coreboard 5/8 Reg.	1/2 Reg., 1/2 Reg.	2-5/8	155	None	140
S9	Shaft	S-4	1 Reg. coreboard, 1 Reg. coreboard	5/8 X, 5/8 X	3-1/4	157	SHT, Spline	124
S10	Shaft	S-5	1 Reg. coreboard, 1 Reg. coreboard	5/8 X, 7/8 Horizontal furring channel, 5/8 X	4-1/8	180	SHT, Spline	140

TABLE 2 (Continued)

			Shaft Side Core	Room Side Core				
Specimen No.	Exposed Surface	Spline Type (See Details, Figure 5)	Wallboard Type and Thickness (in.), Beginning at Surface Membrane	Wallboard Type and Thickness or Spacer and Thickness (in.) Listed in Order of Erection	Total Thickness (in.)	Endurance Time (minutes)	Failure Mode, Location	Time off Wall-board Fall off (minutes)
S11	Shaft	S-5	1 Reg. coreboard, 1 Reg. coreboard	5/8 X	2-5/8	69	SHT, Spline	None
S12	Shaft	S-6	1 Reg. coreboard, 1 Reg. coreboard	5/8 X	2-5/8	131	SHT, Spline	125

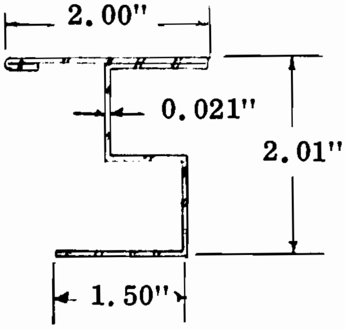

(S-1)

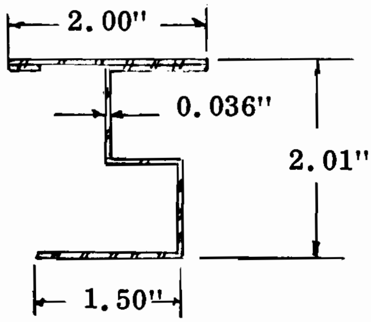

(S-2)

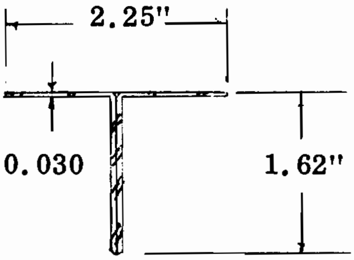

(S-3)

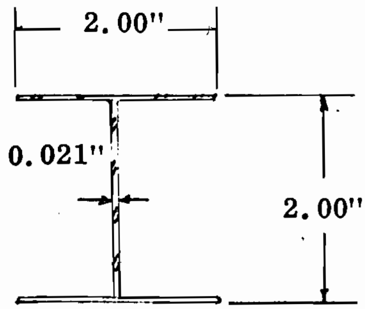

(S-4)

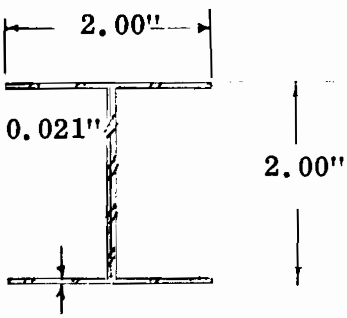

(S-5)

2 channels back to back

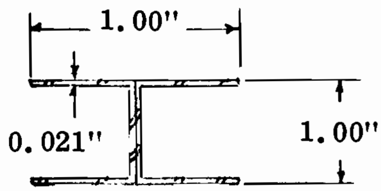

(S-6)

2 channels back to back, staggered each coreboard layer

Figure 5. Spline types

TABLE 3

WALL ASSEMBLIES WITH WOOD STUDS FACED WITH GYPSUM WALLBOARD

Specimen No.	Load Bearing	Exposed Surface Wallboard Type and Thickness (in.)	Nominal Stud Dimensions (in.)	Cavity Material and Thickness (in.)	Unexposed Surface Wallboard Type and Thickness (in.)	Total Thickness (in.)	Endurance Time (minutes)	Failure Criterion, Location	Time of First Wallboard Fall off (minutes)
W1	Yes	1/2 Reg.	2 x 4 Staggered Studs	2 Layers of 3-1/2 Glass fiber insulation	1/2 Reg.	6-1/2	64	LD	36
W2	No	1/2 Reg.	2 x 4	3-1/2 Glass fiber insulation	1/2 Reg.	4-1/2	49	CW, Cavity	35
W3	Yes	1/2 XXX	2 x 4 Staggered Studs	2 Layers of 3-1/2 Glass fiber insulation	1/2 XXX	6-1/2	71	LD	None
W4	Yes	1/2 XXX	2 x 4 Double Studs, Not staggered	3-1/2 Glass fiber insulation	1/2 XXX	9	75	LD	None
W5	Yes	5/8X over 1/2 in. Rigid board insulation	2 x 4	2-5/8 Air space	5/8X over 1/2 in. Rigid board insulation	5-7/8	72	LD	None

TABLE 3

(Continued)

Specimen No.	Load Bearing	Exposed Surface Wallboard Type and Thickness (in.)	Nominal Stud Dimensions (in.)	Cavity Material and Thickness (in.)	Unexposed Surface Wallboard Type and Thickness (in.)	Total Thickness (in.)	Endurance Time (minutes)	Failure Criterion, Location	Time of First Wallboard Fall off (minutes)
W6	Yes	5/8X attached to Furring channels	2 x 4	2-5/8 Air space	5/8 X attached to Furring channels	5-7/8	67	LD	None
W7	Yes	5/8X attached to Furring channels	2 x 4	1-1/2 Glass fiber insulation 1-1/8 Air space	5/8X attached to Furring channels	5-7/8	63	LD	None
W8	Yes	5/8X over 1/2 in. Rigid board insulation	2 x 4	2-5/8 Air space	5/8 X over 1/2 in. Rigid board insulation	5-7/8	68	LD	62
W9	Yes	5/8X over 1/2 in. Rigid board insulation	2 x 4	2-5/8 Air space	5/8 X over 1/2 in. Rigid board insulation	5-7/8	60	No end point	None
W10	No	1/2Reg., 1Reg.	1-5/8x 2	2 Air space	1/2 Reg., 1 Reg.	5	160	SHT Stud	47

CHAPTER 3
HEAT TRANSFER ASPECTS

The development of a method of evaluating the fire resistive qualities of a gypsum wallboard assembly would logically begin by analyzing the heat transfer aspects of the assembly. The three classical modes of heat transfer are conduction, convection, and radiation. Although each mode normally is treated separately in the mathematical analysis of a heat transfer problem, practical engineering applications seldom involve one mode but rather two and sometimes three modes simultaneously.

The simplest approach and most well understood mode of heat transfer is one dimensional conduction under steady-state conditions. This problem involves the transfer of energy from a higher temperature region, T_H, to one of a lower temperature, T_L, over a distance x with T_H, T_L, and the temperature gradient $\frac{dT}{dx}$ constant. The basic law which quantitatively defines heat conduction is attributed to the French mathematician Jean Fourier (1768-1830). With reference to Figure 6, the one dimensional steady - state form of the Fourier law with the temperature gradient measured along the path of energy flux, q, is expressed analytically,

$$q = -k\,A\,\frac{dT}{dx} \tag{1}$$

in which the negative sign is arbitrarily affixed in order that q be positive.[9] The area normal to the heat flow path is A; k is a property of the conducting material termed the thermal conductivity.

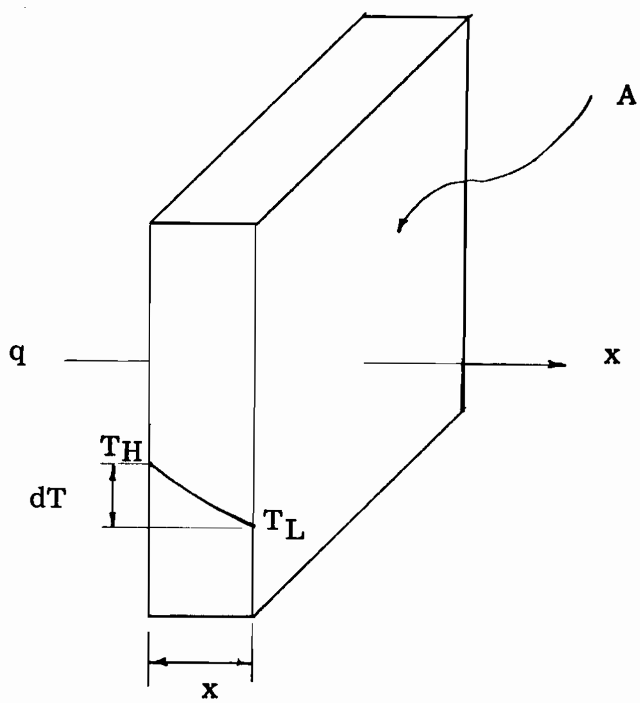

Figure 6. One dimensional steady - state conduction heat transfer

Fire endurance tests are not steady state experiments. Test specimens subjected to the standard ASTM time-temperature fire exposure would have an unexposed surface temperature which is a function of time. Both the temperature gradient $\frac{dT}{dx}$ and the energy flux change with time. A three dimensional mathematical expression for this behavior is the Fourier equation[4]

$$\frac{dT}{dt} = \frac{k}{\rho c_p} \left(\frac{d^2 T}{dx^2} + \frac{d^2 T}{dy^2} + \frac{d^2 T}{dz^2} \right), \tag{2}$$

or

$$\frac{dT}{dt} = \alpha \left(\frac{d^2 T}{dx^2} + \frac{d^2 T}{dy^2} + \frac{d^2 T}{dz^2} \right). \tag{3}$$

Equation (3) is the general heat conduction equation for an isotropic solid with a constant thermal conductivity and describes, in a differential form, the dependence of the temperature in the material on the coordinates x, y, z, and on time, t. The quantity

$$\alpha = \frac{k}{c_p \rho} \tag{4}$$

is the thermal diffusivity, a property of the conducting material for unsteady-state conditions; c_p is the specific heat; ρ is the density of the medium.

The temperature gradient of a test specimen, suddenly subjected to fire on one surface, is initially nonlinear; however, it will gradually become linear and constant if the boundary conditions do not change and if the thermal properties of the material do not vary with time or temperature. This defines a steady state condition; $\frac{dT}{dt} = 0$, and Equation (3) then becomes the Laplace equation[7]

$$\frac{d^2T}{dx^2} + \frac{d^2T}{dy^2} + \frac{d^2T}{dz^2} = 0. \tag{5}$$

To investigate a test specimen subjected to the Standard ASTM Time - Temperature Curve, the unsteady or transient state equation should be solved. An initial assumption is that the thermal conductivity, density, and specific heat are independent of the temperature. If the exposed and unexposed surfaces of the test specimen are considered to have semi - infinite area, the temperature gradients in the y - and z - directions are zero, and Equation (3) yields the one dimensional condition

$$\frac{dT}{dt} = \frac{k}{c_p \rho} \frac{d^2T}{dx^2} \tag{6}$$

or

$$\frac{d^2T}{dx^2} = \frac{1}{\alpha} \frac{dT}{dt} \quad . \tag{7}$$

Equation (7) in partial - differential form has many solutions. The approach treated herein is governed by Duhamel's theorem.[9] Duhamel's theorem can be used for systems with an arbitrary initial temperature distribution, and for cases in which the surface temperature or the temperature of the ambient varies not only with time but with position as well.

In this investigation, the Duhamel method is applied to a system which is assumed to be a semi - infinite solid homogeneous slab of constant thickness, L. The solid is initially at a uniform temperature T_i throughout and at time $t = 0$, its surface $x = 0$ begins to undergo a general temperature change with time $T_1(t)$. In this case the temperature $T(x, t)$ within the solid must satisfy Equation (7) with α constant and the initial and boundary conditions

$$T = T_i \quad \text{at} \quad t = 0, \quad x \geq 0 \, , \tag{8}$$

$$T = T_1 (t) \quad \text{at} \quad x = 0, \quad t > 0 \, .$$

Let $\quad T = u + v;$ (9)

then u and v must likewise satisfy Equation (7) and the simplified set of initial and boundary conditions

$$u = T_i \quad \text{at} \quad t = 0, \quad x \geq 0, \tag{10}$$

$$u = 0 \quad \text{at} \quad x = 0, \quad t > 0,$$

and

$$v = 0 \quad \text{at} \quad t = 0, \quad x \geq 0,$$

$$v = T_1 (t) \quad \text{at} \quad x = 0, \quad t > 0. \tag{11}$$

Figure 7 shows the initial and boundary conditions described by u and v.

Now, consider the Fourier Equation (7). Separation of variables and use of the Fourier sine integral yields the solution

$$u\,(x,\, t) = \frac{2T_i}{\sqrt{\pi}} \int_0^X e^{-w^2}\, dw = T_i \, \text{erf}\,(X)\,, \tag{12}$$

which satisfies the initial and boundary conditions given by (10). The integral in (12) is the error function; its values depend on X, where

$$X = \frac{x}{2\sqrt{\alpha t}} \quad ; \quad w = \frac{n\pi}{L} \quad \text{, where } n = 1, 2, 3, \ldots .$$

The solution for v (x, t) is determined by Duhamel's theorem from the solution for the case in which the initial temperature is zero and the surface temperature is one.[9] Duhamel's theorem states the following:

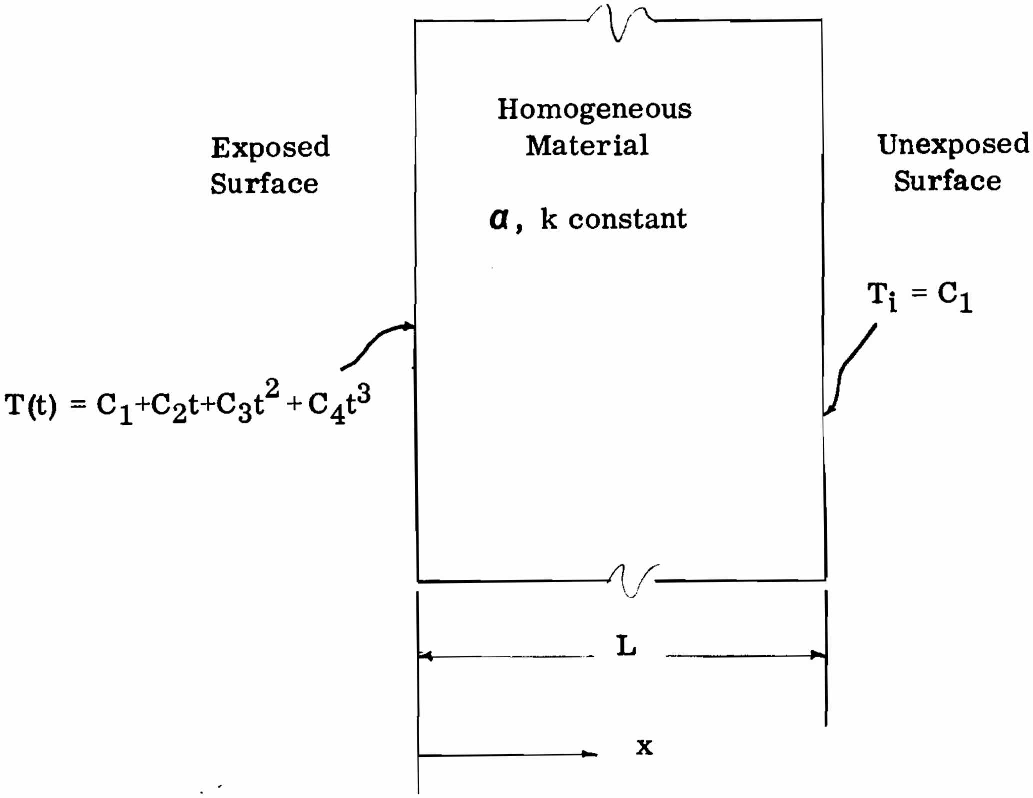

Figure 7. Initial and boundary conditions described by u and v

If f (x, t) is the solution for the temperature history in a solid whose initial temperature is zero, and whose surface is maintained at a temperature of unity, then the solution v (x, t) for the case where its surface is maintained at a transient temperature of T_1 (t) is given by

$$v(x,t) = \int_0^t T_1(w) \frac{d}{dt} f(x, t-w)\,dw. \tag{13}$$

The preliminary solution f (x, t) must satisfy the initial and boundary conditions

$$f = 0 \quad \text{at} \quad t = 0, \quad x \geq 0$$

$$f = 1 \quad \text{at} \quad x = 0, \quad t > 0.$$

The solution $f(x, t) = 1 - \text{erf}(X) = \text{erfc}(X) = \frac{2}{\sqrt{\pi}} \int_X^{\infty} e^{-w^2} dw$

is derived in a manner similar to that of Equation (12). By substituting $(t - w)$ for t, and then taking the partial derivative of $f(x, t - w)$ with respect to t, the solution

$$\frac{d}{dt} f(x, t - w) = \frac{x}{2\sqrt{\pi a}} \frac{e^{-\frac{x^2}{4a(t-w)}}}{(t-w)^{3/2}}$$

is produced. Then applying Duhamel's theorem

$$v(x, t) = \frac{x}{2\sqrt{\pi a}} \int_0^t T_1(w) \frac{e^{-\frac{x^2}{4a(t-w)}}}{(t-w)^{3/2}} dw. \qquad (14)$$

To simplify Equation (14), let $p^2 = \frac{x^2}{4a(t-w)}$.

Then $$v(x, t) = \frac{2}{\pi} \int_{\frac{x}{2\sqrt{at}}}^{\infty} T_1 \left(t - \frac{x^2}{4ap^2} \right) e^{-p^2} dp. \qquad (15)$$

Therefore, $T = u + v$ is the sum of Equations (12) and (15).

For the special case where the temperature history of the exposed surface is assumed to be described by the cubic equation

$$T = C_1 + C_2 t + C_3 t^2 + C_4 t^3,$$

$$v(x, t) = \frac{2}{\pi} \int_X^{\infty} \left[C_1 + C_2 \left(t - \frac{x^2}{4ap^2} \right) + C_3 \left(t - \frac{x^2}{4ap^2} \right)^2 + C_4 \left(t - \frac{x^2}{4ap^2} \right)^3 \right] e^{-p^2} dp. \qquad (16)$$

Now, integrate v (x, t) as given in Equation (16) by parts, where

$$r\ ds = rs - \int s\ dr \quad \text{and} \quad r = e^{-p^2} \text{ in each case.}$$

By combining these results with u (x, t), the temperature profile of the system is given by

$$
\begin{aligned}
T(x,t) = {} & C_1 + C_2 t \left[1 + 2X^2 \operatorname{erfc}(X) - \frac{2}{\sqrt{\pi}} X e^{-X^2} \right] + C_3 t^2 \Bigg[\operatorname{erfc}(X) \\
& - \frac{4}{\sqrt{\pi}} X e^{-X^2} + 4X^2 \operatorname{erfc}(X) \\
& + \frac{2X^4}{3\sqrt{\pi}} \frac{e^{-X^2}}{X^3} - \frac{4X^4}{3\sqrt{\pi}} (E) \Bigg] \\
& + C_4 t^3 \Bigg[\operatorname{erfc}(X) - \frac{6X^2}{\sqrt{\pi}} (E) \\
& + \frac{2Xe^{-X^2}}{\sqrt{\pi}} - \frac{4X^4}{\sqrt{\pi}} (E) \\
& - \frac{2Xe^{-X^2}}{5\sqrt{\pi}} + \frac{4X^3 e^{-X^2}}{15\sqrt{\pi}} - \frac{8X^6}{15\sqrt{\pi}} (E) \Bigg],
\end{aligned}
\tag{17}
$$

where $E = \dfrac{e^{-X^2}}{X} - \sqrt{\pi}\operatorname{erfc}(X).$

The independent variables in Equation (17) are x and t; the dependent variable is the thermal diffusivity α. A value of α may be found for a homogeneous medium, then $T(x, t, \alpha)$ can be determined directly from Equation (17). The constants C_1, C_2, C_3, and C_4 are the coefficients of the assumed cubic equation which defines the temperature history of the exposed surface. This investigation assumes the following values for these coefficients: $C_1 = 70$, $C_2 = 159.167$, $C_3 = -5.500$, $C4 = 0.05833$.

Therefore, $T = 70 + 159.167\,t - 5.500\,t^2 + 0.05833\,t^3$, (18)

where t is the elapsed time of fire exposure in minutes and T is the exposed surface temperature expressed in degrees Fahrenheit. At time $t = 0$, the temperature is 70° F for all x. The area variation of the assumed exposed surface temperature history compared to the area under the Standard ASTM Time - Temperature Curve for furnace temperature control is minus 3.76 percent as calculated with the aid of a computer program regularly used by the Building Research Laboratory.

During a fire test, however, the exposed surface temperature of the specimen is less than the furnace temperature.[8] The temperature decrease is the result of the surface thermal resistance to heat transfer encountered at the boundary surface and is determined by the surface heat transfer coefficient, h. This coefficient is a complicated function of the thermal, physical, and dynamic properties of the conducting system and the ambient medium. Figure 8 shows the temperature profile which may exist during a fire test for a simple single - wall system.

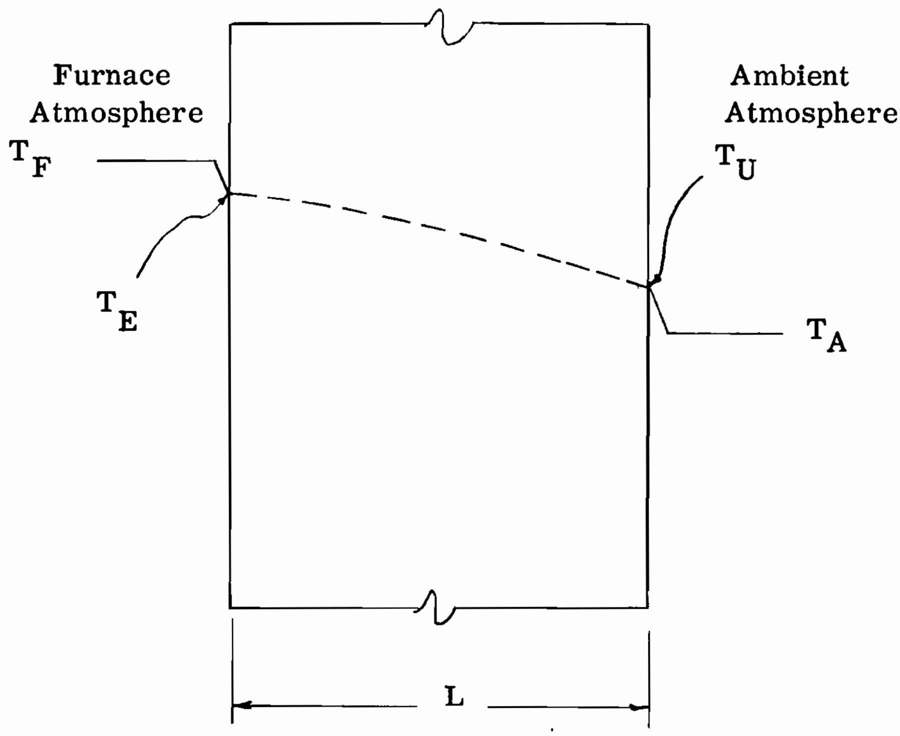

Figure 8. Temperature profile along the path of heat transfer

T_F = Furnace temperature

T_E = Exposed surface temperature

T_U = Unexposed surface temperature

T_A = Ambient temperature

The temperature drop between T_F and T_E must occur in order to induce the heat transfer through the surface resistance film by both the convective and radiative components. The temperature drop between T_U and T_A is the result of resistance to heat transfer encountered at the unexposed surface.

The resistance to conductive heat transfer through the solid wall may be taken as

$$R = \frac{L}{\alpha A} . \tag{19}$$

By assuming A equal to unity, Equation (19) reduces to

$$R = \frac{L}{\alpha} . \tag{20}$$

To account for the surface resistances, α may be reduced to α_r such that the temperature profile may be defined using pure conduction heat transfer as shown in Figure 9.

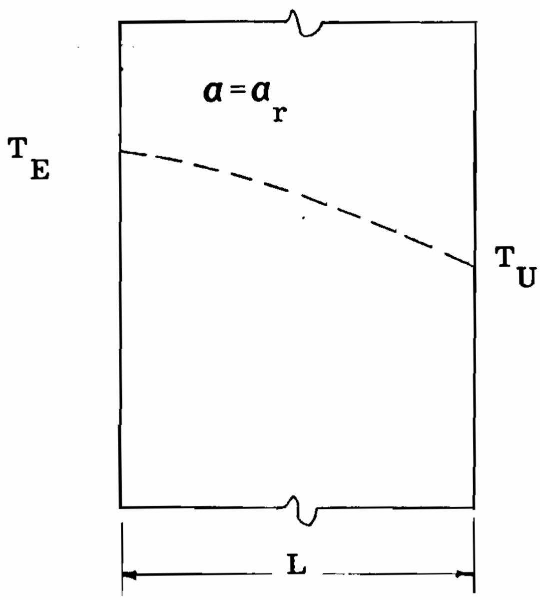

Figure 9. Temperature profile assuming pure conduction heat transfer with negligible surface resistance

An extension of the simple single-wall assembly is the composite wall made up of two or more layers of different materials. A wall construction system commonly is a series composite wall or a parallel composite wall or combinations thereof.

To aid in determining the thermal resistance of the more complex problems involving composite walls, the familiar electrical conduction analogy may be applied. Given a composite wall, an analogous electric circuit may be drawn and the equivalent thermal resistance over the total thickness of the wall system may be obtained by a conventional electrical solution.

A series composite wall and its electrical analogue is shown in Figure 10.

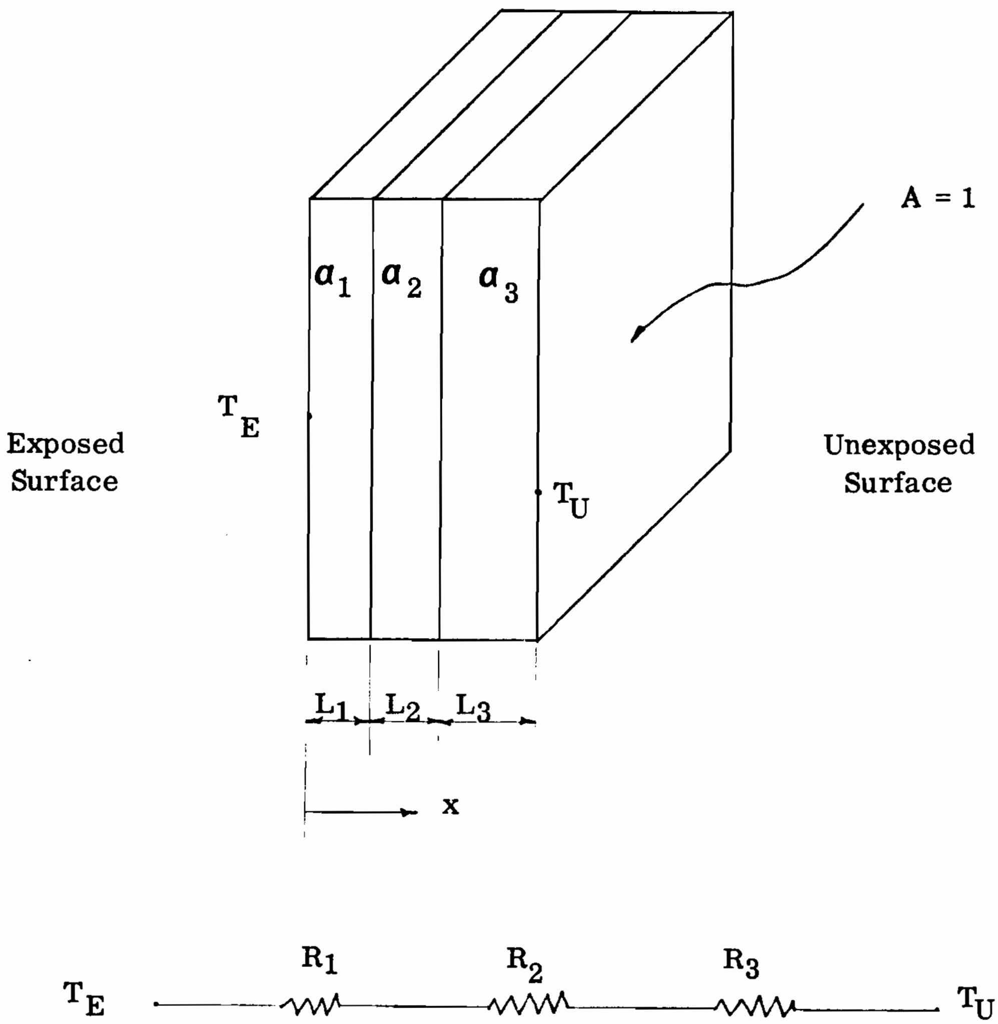

Figure 10. Series composite wall and its electrical analogue

For the case of this series composite wall,

$$R_T = \Sigma R_i = R_1 + R_2 + R_3 \,, \tag{21}$$

or in the form of Equation (20),

$$\frac{L_T}{\alpha_T} = \frac{L_1}{\alpha_1} + \frac{L_2}{\alpha_2} + \frac{L_3}{\alpha_3} \,. \tag{22}$$

This analysis effectively transforms the series composite wall with varying elemental L_i and α_i into a single homogeneous wall of total thickness L_T and mean diffusivity α_T assuming negligible interface contact resistances.

A parallel composite wall and its electrical analogue is shown in Figure 11.

For this parallel composite wall,

$$\frac{1}{R_T} = \Sigma \frac{1}{R_i} = \frac{1}{R_1} + \frac{1}{R_2} + \frac{1}{R_3} \,, \tag{23}$$

or again in the form of Equation (20),

$$\frac{1}{\frac{L_T}{\alpha_T}} = \frac{1}{\frac{L_1}{\alpha_1}} + \frac{1}{\frac{L_2}{\alpha_2}} + \frac{1}{\frac{L_3}{\alpha_3}} \,, \tag{24}$$

where $L_T = L_1 + L_2 + L_3$

In a manner similar to the series analysis, the parallel composite wall is transformed into a single homogeneous wall. For a system similar to that shown in Figure 11, two dimensional heat transfer may result if the thermal conductivities and thus the diffusivities of the materials are significantly different.[4] This condition is accounted for by considering the ratio of the

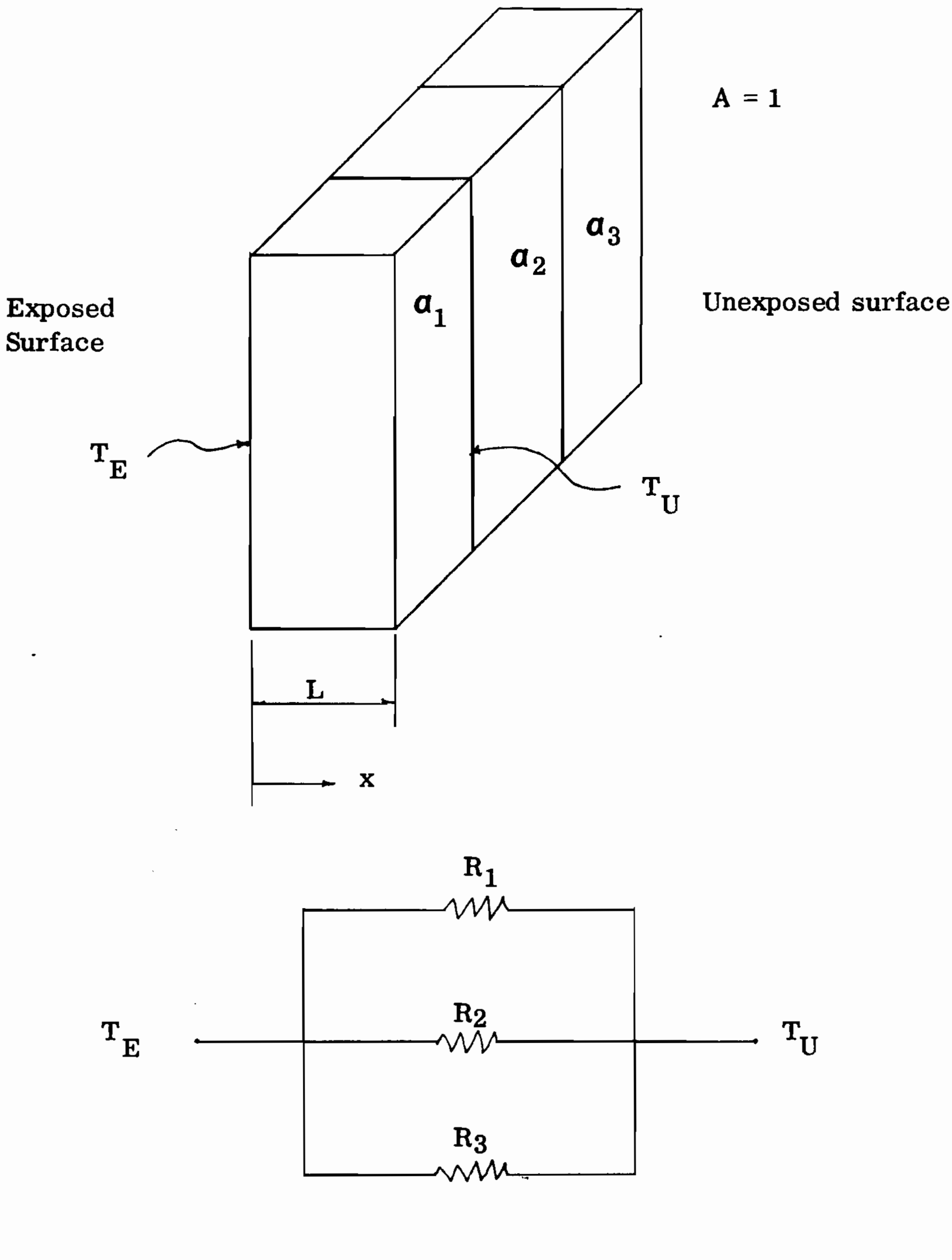

Figure 11. Parallel composite wall and its electrical analogue

cross sectional area perpendicular to the heat flow path in the x - direction to the total area considered in each material. With reference to Figure 11, arbitrarily let

$$\frac{A_1}{A} = \frac{2}{5}, \quad \frac{A_2}{A} = \frac{1}{5}, \text{ and } \quad \frac{A_3}{A} = \frac{2}{5}.$$

Then according to Equation (24),

$$\frac{1}{\frac{L_T}{T}}(1) = \frac{1}{\frac{L_1}{1}}(2/5) + \frac{1}{\frac{L_2}{2}}(1/5) + \frac{1}{\frac{L_3}{3}}(2/5) .$$

Therefore Equation (23) may be rewritten, in part, as

$$\frac{1}{\frac{L_T}{\alpha_T}} = \frac{\frac{A_1}{A}}{\frac{L_i}{\alpha_i}} . \qquad (25)$$

An example of the appication of Equation (25) is demonstrated by a shaft wall assembly with steel splines surrounded by gypsum wallboard. The gypsum wallboard of relatively low thermal conductivity acts as a heat sink for the steel spline material of significantly higher thermal conductivity when the system is subjected to a temperature increase on one surface. Additional discussion of this condition follows later in the text.

A composite wall involving both series and parallel thermal resistances is shown in Figure 12.

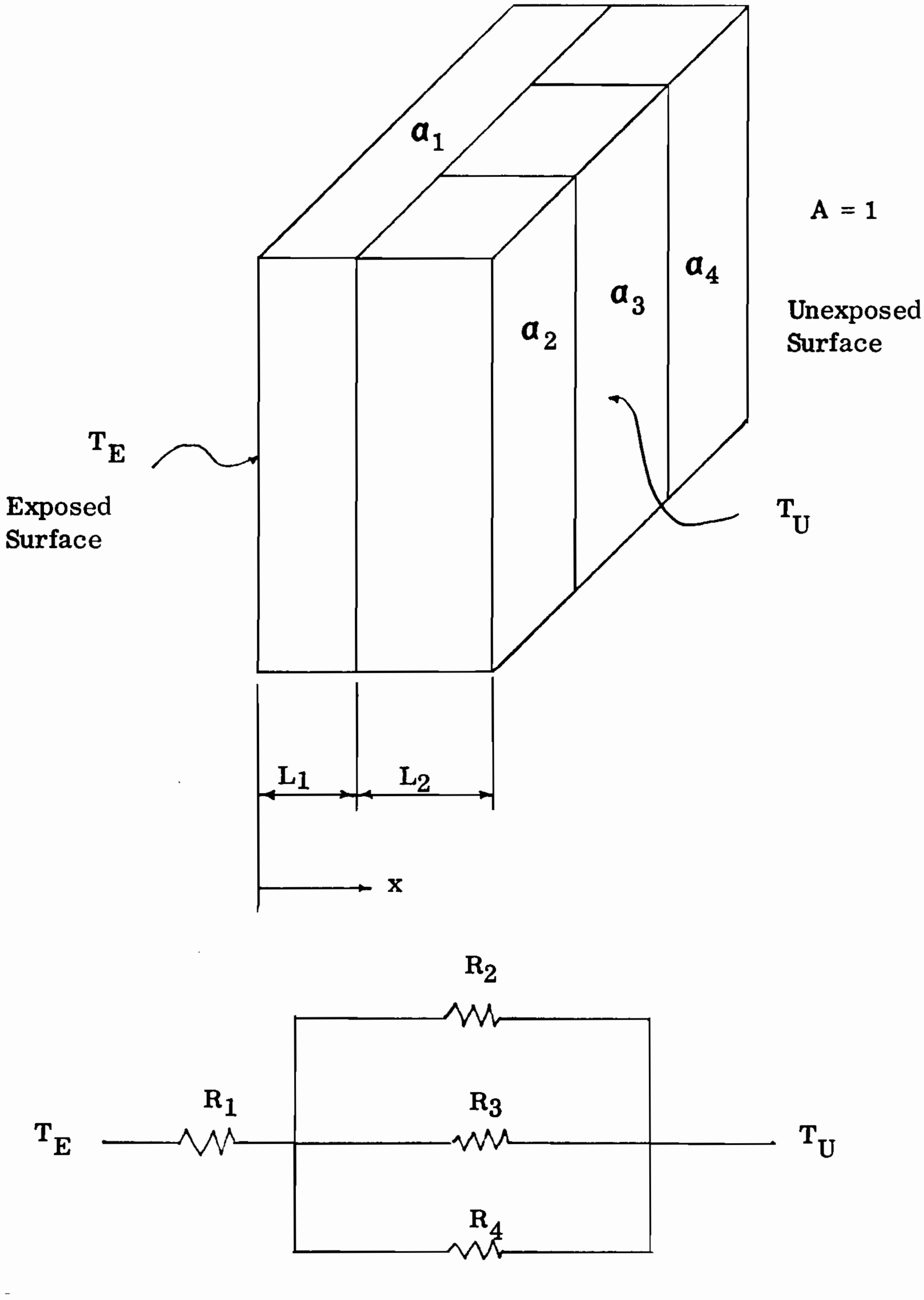

Figure 12. Combination series and parallel wall and its electrical analogue

For this wall, the equivalent thermal resistance is given by

$$R_T = R_1 + \cfrac{1}{\cfrac{A}{R_2A_2} + \cfrac{A}{R_3A_3} + \cfrac{A}{R_4A_4}} \quad (26)$$

The quantity $\frac{L_T}{\alpha_T}$ can be found in a manner similar to the previous two cases.

Hence, for a composite wall system, L_T, α_T and thus a theoretical $T(x, t, \alpha)$ can be determined directly from Equation (17) following transformation of the composite wall to an equivalent homogeneous simple wall.

In addition to previous assumptions, Equation (17) considers the medium to have zero moisture content. Gypsum wallboard, with the exception of the foil - backed variety, has a porous paper surface and core. As a result, gypsum wallboard, as is the case of many other building materials, has a moisture content dependent to a degree upon the relative humidity of the surrounding atmosphere in addition to its chemically combined water. Therefore, not all of the energy that the gypsum receives is transferred to an adjacent area. Large amounts of energy are needed to do the work of raising the temperature of the water contained in the gypsum wallboard. To raise the temperature of 1 lb of water from 63° F to 64° F requires 1 Btu . The amount of heat per unit mass necessary to change a liquid to the vapor phase without a change in temperature is called the heat of vaporization. The heat of vaporization of water is approximately 970 Btu per lb at atmospheric pressure. This is over five times as much energy as is needed to raise the temperature of water from 32° F to 212° F.

A clearly defined temperature lag exists when a construction assembly containing water is subjected to a fire endurance test. In the case of water, the lag occurs when the temperature at a specific point within the test specimen reaches 212° F. When this happens, a temperature plateau is maintained as the water is changed into vapor. Some of the vapor is transmitted from the region through the permeable material in the direction of the energy flow. Nevertheless, the temperature of that region will remain at approximately 212° F until there is no moisture in that segment. At this point, the temperature again begins to rise.

Fire tests in which thermocouples are positioned within the stud cavities of wall assemblies with membranes containing moisture have shown a definite 212° F plateau. Those assemblies with the thicker membranes have a longer duration of leveling temperature due both to a larger amount of moisture present and to the lower temperature gradient which exists during fire exposure. Harmathy[5] has discussed the effect of moisture content on the fire endurance of building elements. The previously mentioned reduction of the mean diffusivity of the gypsum wallboard accounts, in part, for the temperature lag which exists in the theoretical computation of the unexposed surface temperature history given in Equation (17). An alternate to the reduction of the diffusivity could have been the introduction into the equation of a negative equivalent temperature rise before the resumption of the temperature rise subsequent to the 212° F plateau. This negative temperature rise would be a function of the moisture content, permeability, and the temperature gradient of the medium.

The protrusion of the fasteners through the gypsum wallboard membrane into the stud or, less frequently, into another layer of wallboard is not considered in determining the mean diffusivity for substitution into Equation (17). Instead, a unit area of the specimen is considered where a fastener does not exist. If the effect of a fastener were analyzed, a parallel electrical analogue would have been the primary tool in a solution for the mean diffusivity of the fastener-free equivalent wall system.

Additional assumptions in the evaluation of the gypsum wallboard assemblies are treated under separate discussion when the different categories of wall assemblies are considered in the following chapter.

CHAPTER 4

A STUDY OF THE THEORETICAL AND FIRE TEST RESULTS OF THE WALL ASSEMBLIES

The basis for the study of the theoretical and fire test results of the wall assemblies is the unexposed surface temperature as a function of time. The unexposed surface temperature history of the fire test specimens is found from the fire test data contained in the project files and the test reports issued by the Building Research Laboratory. The theoretical unexposed surface temperature is taken to be described by Equation (17) given in Chapter 3.

The numerical values for the mean thermal diffusivity of the wall materials are as follows:

Material	Mean thermal diffusivity ($in.^2/hr$)
gypsum wallboard	1.37

Material	Mean thermal diffusivity (in.^{2}/hr)
steel studs and splines	72.00[4]
wood studs	0.57[4]
air	175.00[3]
building insulation	175.00[3]

The mean thermal diffusivity of air and building insulation is assumed to be the value for air at 200°F. The identical value for thermal diffusivity of building insulation is explained later in this chapter. The thermal diffusivity of wood varies little among the softwood species. The value for steel is taken for 0.5 percent carbon steel at a temperature of approximately 400°F. The value for the thermal diffusivity of the gypsum wallboard is near the lower limit in the range of temperature dependent values given by Harmathy and Krokosky.[7] The relatively low value reflects the additional resistance to heat transfer which occurs at the wallboard surfaces and the effect of the emmission of steam from the gypsum wallboard at temperatures above 212°F. The remaining terms in Equation (17) are previously defined.

Similar to Chapter 2, the analysis of the steel stud partitions, the steel spline shaft walls and the wood stud walls are studied separately due to the inherent differences in materials and construction.

The typical steel stud partition assembly is a series composite wall. Figure 13 shows a cross section of a typical steel stud partition assembly.

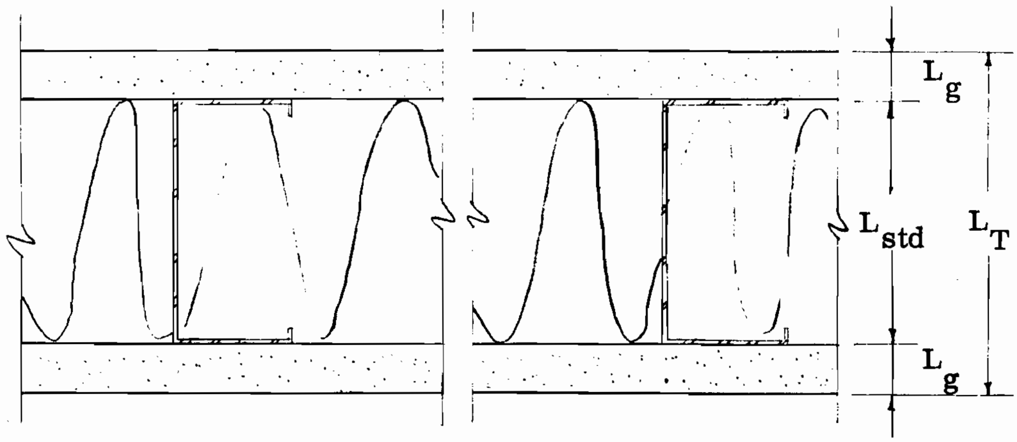

Figure 13. Cross section of a steel stud partition assembly

The unit area of the wall normal to the assumed unidirectional heat flow path is taken at the stud location. As shown in Table 1, the steel stud location was primarily the site at which the first ASTM failure criterion was reached. The thermal resistance of the partition assembly is determined from the series analogue solution of the component thermal resistance of the exposed surface wallboard, the steel stud, and the unexposed surface wallboard. Therefore, the equivalent thermal resistance of the transformed homogeneous wall is given by

$$R_T = \Sigma R_i ; \tag{21}$$

or for the assembly described above and shown in Figure 13,

$$\frac{L_T}{\alpha_T} = \frac{L_g}{\alpha_g} + \frac{L_{std}}{\alpha_{std}} + \frac{L_g}{\alpha_g} ;$$

where L_g = thickness of gypsum wallboard, L_{std} = depth of stud, α_g =

thermal diffusivity of gypsum wallboard, and α_{std} = thermal diffusivity of the stud.

Table 4 lists the unexposed surface temperature data from the fire endurance tests and the theoretical thermal properties determined by the series analogue analysis of the P-series test specimens. Figure 14 is a graph showing L_T versus α_T for the P-series test specimens. Adjacent to each data point is the Fire Endurance Time of that assembly in minutes. Straight line curves are drawn to depict α_T and L_T coordinates which appear to represent values for the Fire Endurance Times of 60, 90, 120, and 150 minutes. The 90 minute curve is interpolated from the 60 and 120 minute curves due to lack of data points. Therefore, the 90 minute curve should be given less reliance than that of the other curves. Similarly, the coordinates α_T and L_T would be more reliable in the range of values represented by the test specimens than those values depicted by the curves beyond the test specimen α_T, L_T range.

The steel spline shaft wall assembly is an example of a combination series and parallel composite wall. Figure 15 shows a cross section of a typical shaft wall assembly with an illustration of the shaft side core and the room side core. The shaft side core is the parallel composite portion of the assembly. The shaft side core consists of the steel splines surrounded either partially or completely by gypsum wallboard. The room side core consists of one or more layers of gypsum wallboard with occasional use of

TABLE 4

TEMPERATURE DATA AND THERMAL PROPERTIES OF PARTITION ASSEMBLIES WITH STEEL STUDS FACED WITH GYPSUM WALLBOARD

Specimen No.	Elapsed Time, t (minutes)	Avg. Unexposed Surface Temp-erature (° F)	Avg. Unexposed Surface Temp-erature at Stud Cavity (° F)	Unexposed Surface Temperature at the Stud Locations (° F)			L_T, α_T (in., in.^{2}/hr	Theoretical T (° F) at Time t, from Equation (17)
				Low	Average	High		
P1	60	284	241	239	328	399	3.50, 4.57	376
P2	61	307	271	297	360	447	3.50, 4.57	407
P3	60	286	266	258	316	375	2.50, 3.32	494
P4	60	172	171	165	174	180	4.00, 2.72	167
P5	60	213	208	215	220	223	5.12, 4.48	168
P6	60	256	214	238	297	350	3.75, 3.96	291
P7	60	307	299	290	335	380	3.75, 3.96	291
P8	60	255	222	245	330	385	3.00, 3.20	361
P9	60	303	322	235	275	300	4.88, 5.07	217
P10	60	257	261	230	251	280	3.50, 5.00	405

TABLE 4 (Continued)
TEMPERATURE DATA AND THERMAL PROPERTIES OF PARTITION ASSEMBLIES WITH STEEL STUDS FACED WITH GYPSUM WALLBOARD

Specimen No.	Elapsed Time, t (minutes)	Avg. Unexposed Surface Temp-erature (° F)	Avg. Unexposed Surface Temp-erature at Stud Cavity (° F)	Unexposed Surface Temperature at the Stud Locations (° F)			L_T, α_T (in., in^2/hr)	Theoretical T (° F) at Time t, from Equation (17)
				Low	Average	High		
P11	60	235	226	240	255	285	4.00, 3.28	208
P12	60	167	163	165	172	185	4.50, 3.00	143
P13	60	249	248	245	252	260	2.88, 3.08	376
P14	60	242	241	235	243	250	4.88, 5.07	217
P15	60	175*				180*	5.75, 3.61	104
P16	60	170*				200*	5.75, 3.61	104
P17	60	169	152	165	170	175	4.50, 3.00	143
P18	60	182	173	170	200	230	5.50, 3.54	111
P19	60	136	136	130	135	140	8.50, 4.37	73
P20	60	219	218	205	220	240	3.75, 3.96	291

*Values taken from fire test report graph

TABLE 4 (Continued)
TEMPERATURE DATA AND THERMAL PROPERTIES OF PARTITION ASSEMBLIES WITH STEEL STUDS FACED WITH GYPSUM WALLBOARD

Specimen No.	Elapsed Time, t (minutes)	Avg. Unexposed Surface Temperature (° F)	Avg. Unexposed Surface Temperature at Stud Cavity (° F)	Unexposed Surface Temperature at Stud Locations (° F)			L_T, α_T (in., in.^{2}/hr)	Theoretical T (° F) at Time t, from Equation (17)
				Low	Average	High		
P21	60	159	160	155	158	160	5.00, 2.69	102
P22	60	154	156	150	152	155	6.12, 3.26	86
P23	60	269	248	245	300	355	4.88, 5.07	217
P24	60	249	231	235	310	385	4.88, 5.07	217
P25	60	171	179	165	168	170	6.12, 3.26	86
P26	60	251	248	240	258	295	2.88, 3.08	376
P27	60	231	226	225	243	280	4.88, 5.07	217
P28	60	243	234	245	252	265	3.75, 3.96	291

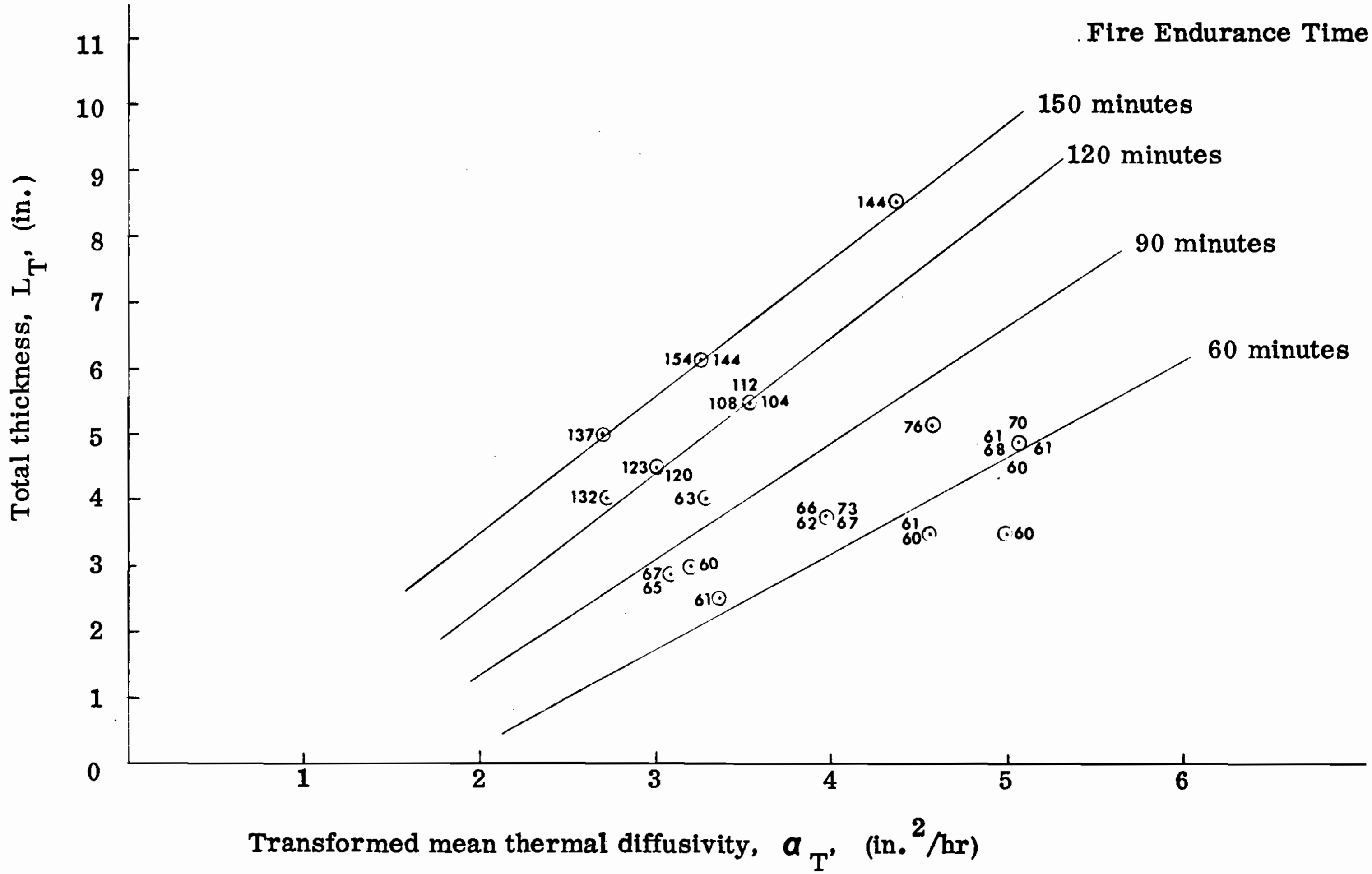

Figure 14. L_T versus α_T for steel stud partitions

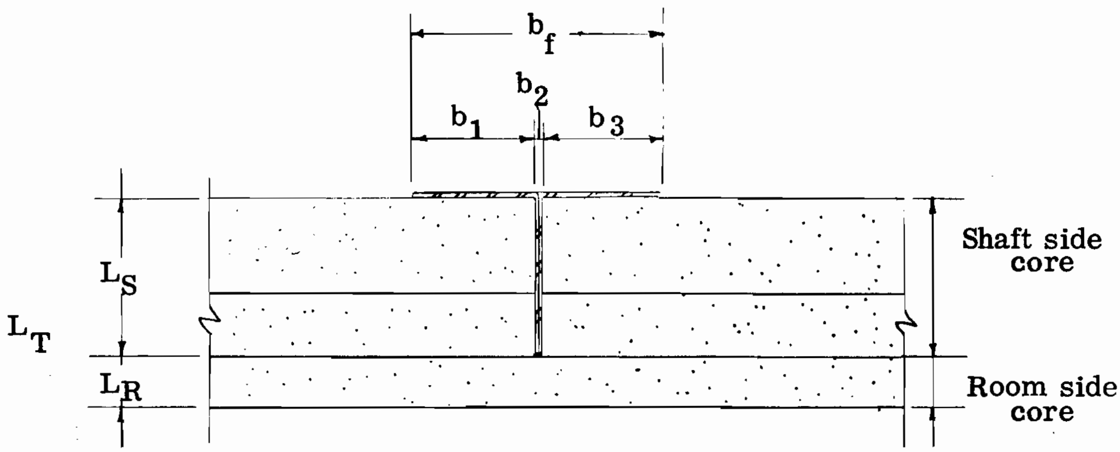

Figure 15. Cross section of a typical steel spline shaft wall assembly

steel furring channels for attachment of the wallboard. Similar to the steel stud partition assembly, the first ASTM failure criterion of the shaft wall assembly tends to occur at the steel spline location as demonstrated in Table 2.

The theoretical thermal resistance of the shaft side core is governed by Equation (25),

$$\frac{1}{\frac{L_S}{\alpha_S}} = \frac{\frac{A_i}{A}}{\frac{L_i}{\alpha_i}}$$

where $\frac{L_S}{\alpha_S}$ is the thermal resistance of the shaft side core. $\frac{A_i}{A}$ is the ratio of the i-component width to the width of the spline flange. With reference to Figure 15,

$$\frac{1}{\frac{L_S}{\alpha_S}} = \frac{\frac{b_1}{b_f}}{\frac{L_1}{\alpha_1}} + \frac{\frac{b_2}{b_f}}{\frac{L_2}{\alpha_2}} + \frac{\frac{b_3}{b_f}}{\frac{L_3}{\alpha_3}}$$

where $\alpha_1 = \alpha_3 = \alpha_g$; $\alpha_2 = \alpha_{std}$; and $L_1 = L_2 = L_3 = L_S$.

The theoretical thermal resistance of the materials which comprise the room side is determined by a series analogue analysis. For this case

$$\frac{L_R}{\alpha_R} = \frac{L_R}{\alpha_g} \quad ;$$

and the equivalent thermal resistance of the transformed homogeneous wall is given by

$$R_T = \Sigma R_i = \frac{L_T}{\alpha_T} = \frac{L_S}{\alpha_S} + \frac{L_R}{\alpha_R} \quad ;$$

where $L_T = L_S + L_R$.

Table 5 lists the unexposed surface temperature data from the fire endurance tests and the theoretical thermal properties determined by the combination series and parallel analogue analysis of the S-series test specimens. Figure 16 is a graph showing L_T versus α_T for the S-series test specimens. Adjacent to each data point is the Fire Endurance Time of that assembly in minutes. Straight line curves are drawn to depict α_T and L_T coordinates which appear to represent values for Fire Endurance Times of

TABLE 5

TEMPERATURE DATA AND THERMAL PROPERTIES OF STEEL SPLINE SHAFT WALL ASSEMBLIES LINED WITH GYPSUM WALLBOARD

Specimen No.	Elapsed Time, t (minutes)	Avg. Unexposed Surface Temperature (°F)	Avg. Unexposed Surface Temperature at Stud Cavity (°F)	Unexposed Surface Temp. at the Stud Locations (°F)			L_T, α_T (in., $in.^2$/hr)	Theoretical T (°F) at Time, t, from Equation (17)
				Low	Average	Hign		
S1	60	177	173	176	182	189	3.00, 2.06	234
S2	60	180	173	202	210	217	3.00, 2.06	234
S3	60	166	165	162	168	175	3.25, 2.24	216
S4	60	155	154	153	156	161	3.88, 2.03	129
S5	60	169	165	165	174	183	3.00, 2.06	234
S6	60	168	165	168	176	185	3.25, 2.24	216
S7	60	179	174	185	190	199	2.25, 1.94	385
S8	60	160	160	157	159	161	2.62, 1.83	269
S9	60	147	135	169	175	180	3.25, 1.66	153
S10	60	141	143	132	140	152	4.12, 2.38	128

TABLE 5 (Continued)

TEMPERATURE DATA AND THERMAL PROPERTIES OF STEEL SPLINE SHAFT WALL ASSEMBLIES LINED WITH GYPSUM WALLBOARD

Specimen No.	Elapsed Time, t (minutes)	Avg. Unexposed Surface Temperature (°F)	Avg. Unexposed Surface Temperature at Stud Cavity (°F)	Unexposed Surface Temp. at the Stud Locations (°F)			L_T, α_T (in., in^2/hr)	Theoretical T (°F) at Time, t, from Equation (17)
				Low	Average	High		
S11	60	180	160	217	227	236	2.62, 2.07	310
S12	60	163	157	160	171	179	2.62, 1.71	257

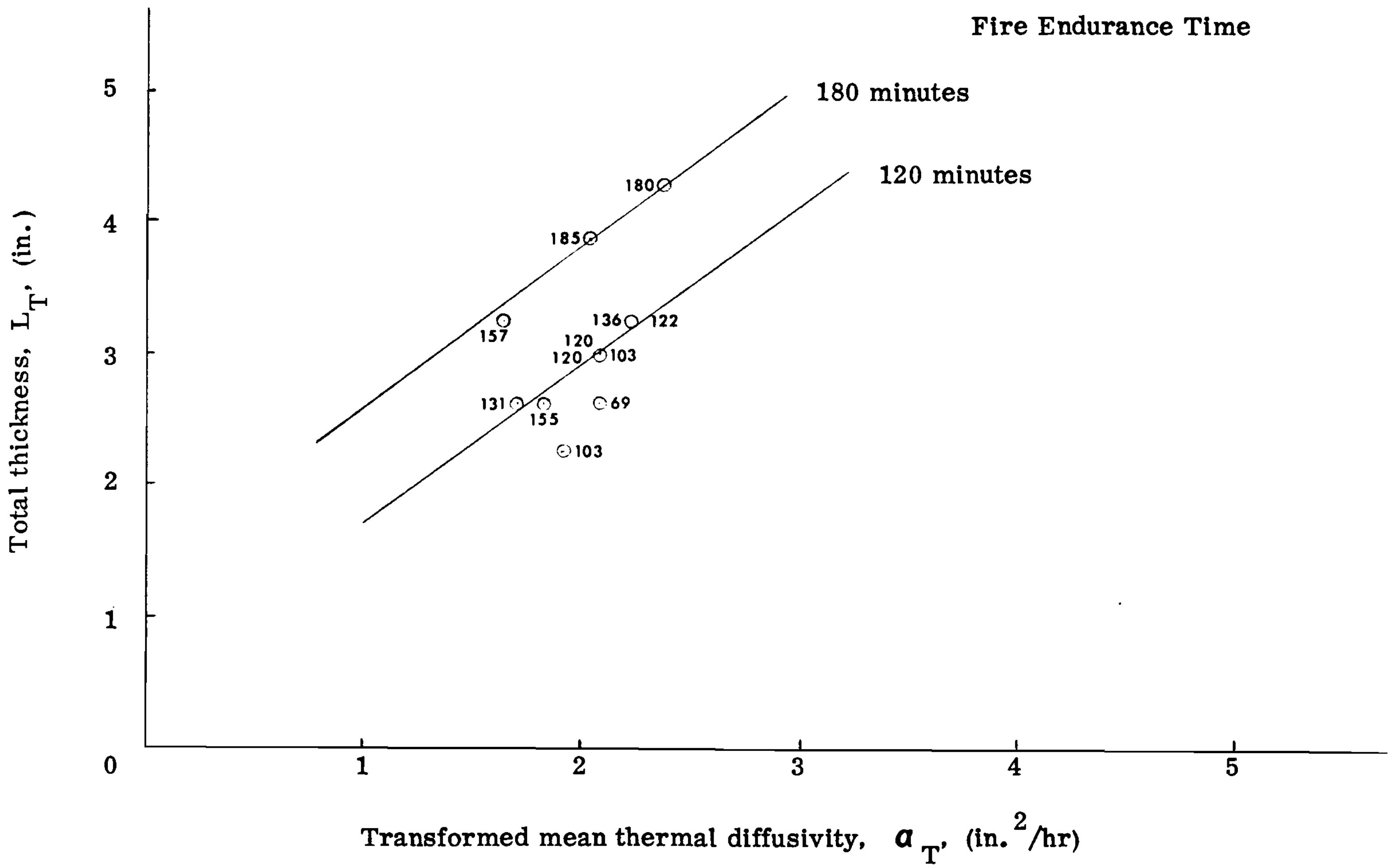

Figure 16. L_T versus α_T for steel spline shaft walls

120 and 180 minutes. As was the case for the steel stud assemblies, the coordinates α_T and L_T would be more reliable in the range of values represented by the test specimens than those values beyond the specimen α_T, L_T range. The coordinates for the 120 minutes curve are similar to those of the steel stud partition assembly.

The wood stud wall assembly is an example of a series composite wall. Figure 17 shows a cross section of a typical wood stud wall assembly.

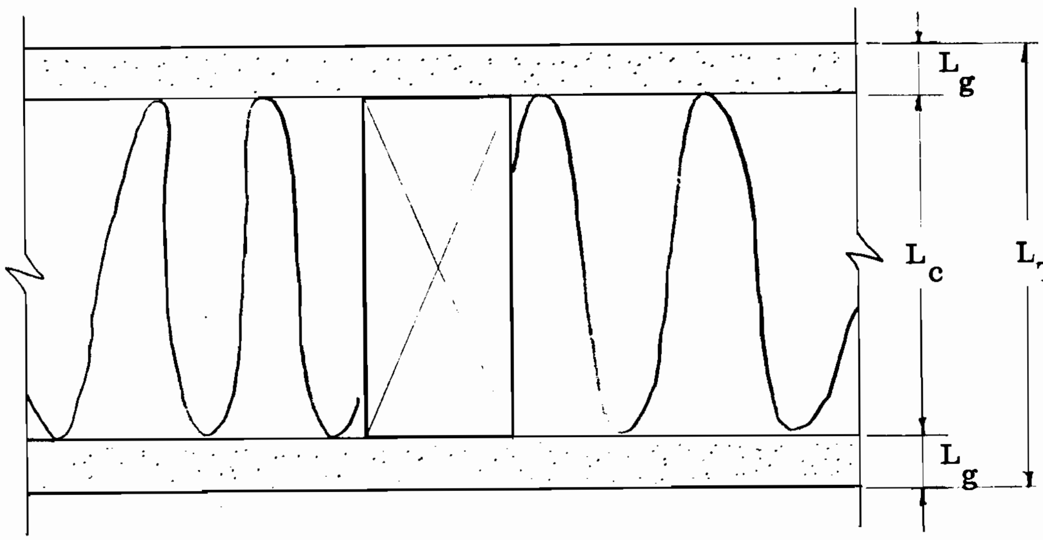

Figure 17. Cross section of a typical wood stud wall assembly

The wood stud wall assembly may be either a non-load bearing partition or a load bearing wall. The application of a load to a wood stud assembly would not directly affect the thermal transmission of the assembly. However, the larger deflection of the load bearing wall due to the applied load coupled with a deterioration of the wood stud may result in increased separation of the wall-board panel joints. The joint separation would expose that portion of the assembly in the vicinity of the stud to a higher temperature than that of a joint which remains intact. Wallboard fall off would increase the thermal transmission for the same reason. Nevertheless, the thermal resistance analysis of both load bearing and non-load bearing assemblies is assumed to be identical.

An inspection of Table 3 shows, that for those assemblies which do not fail under load, the first ASTM failure criterion is usually a single high temperature on the unexposed surface occurring over the stud cavity. Table 6 lists the unexposed temperature data from the W-series fire endurance tests and the theoretical temperature calculated from Equation (17) by the series analogue method. The fire test data in Table 6 gives more evidence that higher unexposed surface temperatures are encountered over the stud cavity than over the stud. Thus, the assumed unidirectional heat flow path across the stud cavity will be investigated. The stud cavity may be either building insulation or air space, or both.

The temperature conditions in the stud cavity are not as well understood as those of the series analysis of the steel stud partition assembly for which material contact is assumed. Likewise the combination series and parallel analysis of the steel spline shaft wall also assumes material contact. The building insulation may be considered to consist of small air spaces surrounded by solid walls. The low conductivity of such materials at room temperature is attributed to the low thermal conductivity of the air enclosed

TABLE 6

TEMPERATURE DATA AND THERMAL PROPERTIES OF WOOD STUD WALL ASSEMBLIES FACED WITH GYPSUM WALLBOARD

Specimen No.	Elapsed Time, t (minutes)	Avg. Unexposed Surface Temperature (° F)	Avg. Unexposed Surface Temperature at Stud Locations (° F)	Unexposed Surface Temperature at the Stud Cavities			L_T, α_T (in., in²/hr)	Theoretical T (° F) at Time t, from Equation (17)
				Low	Average	High		
W1	60	174	148	164	186	217	6.50, 8.53	204
W2	45	196	185	147	207	251	4.50, 6.13	225
W3	60	165	146	151	177	199	6.50, 8.53	204
W4	60	176	137	168	193	206	9.09, 11.60	138
W5	60	172	170	170	177	185	5.88, 6.32	183
W6	60	217	220	175	216	255	5.88, 6.20	179
W7	60	207*				230*	5.88, 6.20	179
W8	60	150	145	140	151	160	5.88, 6.32	183

*Values taken from fire test report graph

TABLE 6 (Continued)
TEMPERATURE DATA AND THERMAL PROPERTIES OF WOOD STUD WALL ASSEMBLIES FACED WITH GYPSUM WALLBOARD

Specimen No.	Elapsed Time, t (minutes)	Avg. Unexposed Surface Temperature (° F)	Avg. Unexposed Surface Temperature at Stud Locations (° F)	Unexposed Surface Temperature at the Stud Cavities			L_T, a_T (in., in.^{2}/hr)	Theoretical T (° F) at Time t, from Equation (17)
				Low	Average	High		
W9	60	175*				180*	5.88, 6.32	183
W10	60	146		140	146	150	5.00, 2.28	89

*Values taken from fire test report graph

within the interstices or cells of the material and the relatively small area of solid material through which the heat may be conducted. For the higher temperatures which are experienced during fire tests, convection currents may arise within the air spaces. For all such materials, the higher the temperature the higher will be the conductance. Heat radiation through the gaseous air apaces or cells will occur and there will be an increase in conductance due to internal convection.

Likewise convection and radiation plays an important role in the stud cavities consisting of air spaces only. Since similar conditions exist in insulation filled cavities and stud cavities with air spaces, the two will be assumed to be identical in a series analogue analysis of the wood stud assembly. The mean thermal diffusivity of the air space is taken to be the thermal diffusivity of air at 200°F. Thus,

$$\alpha_{air} = \alpha_{insulation} = \frac{k}{\rho c_p} = \frac{.0182}{(.241)(.0620)}$$

$$= 1.22 \text{ ft}^2/\text{hr}$$

$$= 175 \text{ in.}^2/\text{hr}$$

For a comparison, the mean diffusivity of wood is approximately 0.004 ft^2/hr or 0.57 in.^{2}/hr. The series analysis is applied to the materials other than the cavity materials in a manner similar to the P-series and S-series fire test specimens. Thus, the values of L_T and α_T in Table 6 reflect the series electrical analogue resistance approach and are computed at the stud cavity area. In Figure 17, L_c denotes the thickness of the stud cavity.

Figure 18 is a graph showing L_T versus a_T for the W-series test specimens. Adjacent to each data point is the Fire Endurance Time of that assembly in minutes. A straight line curve is drawn to depict a_T and L_T coordinates which appear to represent values for a Fire Endurance Time of 60 minutes. No attempt was made to draw additional curves, because excessive error would result from extrapolation. Again, the coordinates a_T and L_T would be more reliable in the range of values represented by the test specimens than those values depicted by the curves beyond the test specimen a_T, L_T range.

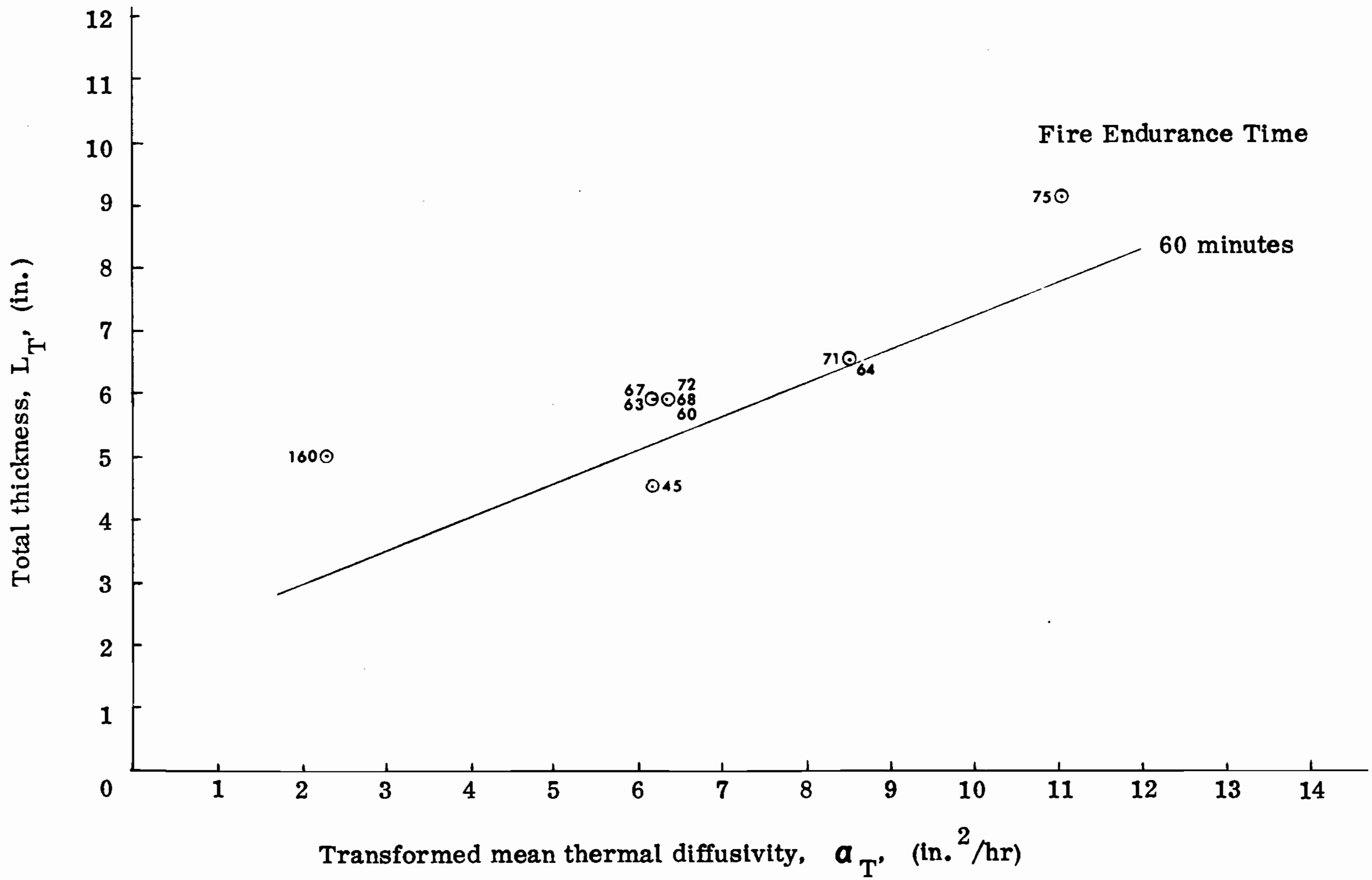

Figure 18. L_T versus α_T for wood stud walls

CHAPTER 5
A DISCUSSION OF RESULTS AND CONCLUSIONS

The unexposed surface temperature history calculated by Equation (17) is an approximation of the temperatures yielded by fire endurance tests. The temperatures given by Equation (17) for the P-series and the S-series specimens were more accurate for a wall thickness in the range of 3 in. to 4 in. than for thicknesses beyond this range. Unexposed surface temperatures were generally overestimated for a wall thickness less than 3 in. and underestimated for a thickness greater than 4 in. The fire test results indicate that the higher unexposed surface temperatures were experienced over the steel studs and splines than over the stud cavities for the P-series and S-series specimens, respectively.

With the assumptions given in the W-series analysis, the theoretical equation yields temperatures near those temperatures encountered in the fire tests. If unidirectional heat conduction were assumed across the wood stud for which the thermal diffusivity is less than gypsum wallboard, Equation (17) produces theoretical temperatures far less than the fire test results. The fire test results, however, show that the unexposed surface temperature over the wood studs were slightly less than the temperatures over the stud cavities with an assumed thermal diffusivity over 100 times greater than gypsum wallboard. This indicates that three-dimensional rather than one-dimensional heat transfer conditions exist during the fire exposure. This was demonstrated to a lesser degree for the P-series and S-series tests.

Another shortcoming of the theoretical equation is its inability to sufficiently account for the 212° F temperature lag. The 212° F temperature plateau is particularly significant in the shaft wall assemblies, characterized by compact multiple layers of water containing wallboard. This shortcoming and others produced by the multiplicity of assumptions given by this study require further investigation.

The theoretical model does aid in generating a family of curves depicting Fire Endurance Times. When values of α_T and L_T determined by the electrical analogue approach are substituted in Equation (17), temperatures inconsistent with those assemblies demonstrating approximately the same Fire Endurance Time indicates that either the analogue analysis was inaccurate or premature failure of the assembly occurred. Therefore, that data point is given less reliance. More test data is needed to produce better defined curves and to extend the range of α_T and L_T values.

Future Research Recommendations

Further investigation of the fire resistive qualities of wall assemblies with gypsum wallboard membranes is needed to examine the fire test conditions and heat transfer mechanisms which were considered in this study by simplifying assumptions. Particular attention should be given to the following: (a) the determination of the surface thermal resistance to heat transfer encountered at the boundary surfaces and the application of the heat transfer coefficient, h, of the test components; (b) the effect of moisture content and the temperature dependency of the thermal diffusivity of gypsum wallboard and other pertinent construction materials; and (c) additional examination with possible alternatives to the series and parallel electrical analogue approach to the transformation of the composite wall assemblies into simple homogeneous walls.

BIBLIOGRAPHY

1. "ASTM Standard Methods of Fire Tests of Building Construction and Materials E 119-71," 1971 Book of Standards ASTM, American Society for Testing Materials, Part 14, 1971.

2. Bletzacker, Richard W., Lane, William W. and Denning, David W., "Fire Resistance of Construction Assemblies," Report No. EES 245, Building Research Laboratory, Engineering Experiment Station, The Ohio State University, December, 1969.

3. Brown, Aubrey I. and Marco, Salvatore M., Introduction to Heat Transfer, Third Edition McGraw-Hill Book Company, Inc., New York, 1958.

4. Chapman, Alan J., Heat Transfer, Second Edition, The Macmillan Company, New York, 1967.

5. Harmathy, T. Z., "Effect of Moisture on the Fire Endurance of Building Materials," Advance Copy of Paper Presentation, American Society for Testing and Materials, Philadelphia, 1964.

6. Holman, J. P., Heat Transfer, McGraw-Hill Book Company, Inc., New York, 1963.

7. Krokosky, Edward M., "Fire Intensity-Resistance Evaluation," Journal of the Structural Division, ASCE, Vol. 96, No. ST11, November, 1970.

8. Krokosky, Edward M., "An Analog Simulator for Evaluating Materials Subjected to the Standard ASTM Fire Curve," Journal of Materials, American Society for Testing and Materials, Vol. 2, No. 4 4, December, 1967.

9. Schneider, P. J., Conduction Heat Transfer, Addison-Wesley Publishing Company, Inc., Reading, 1955.